A FINE ATMOSPHERIC ANALYSIS OF
THE STAR THETA URSAE MAJORIS

By

JOHN G. BULMAN

Bachelor of Science
East Central State College
Ada, Oklahoma
1959

Master of Science
Oklahoma State University
Stillwater, Oklahoma
1964

Submitted to the Faculty of the Graduate College
of the Oklahoma State University
in partial fulfillment of the requirements
for the Degree of
DOCTOR OF EDUCATION
May, 1971

A FINE ATMOSPHERIC ANALYSIS OF

THE STAR THETA URSAE MAJORIS

Thesis Approved:

Leon W. Schroeder
Thesis Adviser

Delbert L. Rutledge

Robert T. Alciatore

[illegible]

D. D. Durham
Dean of the Graduate College

PREFACE

This dissertation is concerned with performing a detailed fine atmospheric analysis of the atmosphere of the star Theta Ursae Majoris using a detailed computer program which computes a pressure opacity-flux model for a given temperature distribution. A grid of sixteen model atmospheres with scaled solar-type distribution was computed for a range of effective temperatures ($6200\ ^{o}K \leq T_{eff} \leq 6650\ ^{o}K$), surface gravities ($3.8 \leq \log g \leq 4.4$), and the solar abundance (log of the summation of the number of hydrogen atoms divided by the number of metal atoms = 3.23, and the number of helium atoms divided by the number of hydrogen atoms = 0.1250).

Theoretical UBV colors, corrected for line blanketing, were computed for each model and compared to observed values in order to determine if a model can be selected as representing the star Theta Ursae Majoris.

Hydrogen line profiles, $H\alpha$, $H\beta$, $H\gamma$, and $H\delta$, for each of the models were computed and compared to the observed profiles. The hydrogen line profiles will also be used to select a model atmosphere for the star. In addition, the model dictated by the UBV colors will be compared with the model dictated by the hydrogen line profiles in order to determine if the selected models are the same or if the UBV colors selects a model having a higher or lower temperature than the model predicted by the hydrogen line profiles.

I wish to express my sincere gratitude to Dr. L. W. Schroeder, my adviser, for his suggestion of the topic, and whose invaluable guidance and encouragement have been most valuable in the preparation of this thesis.

I would like to thank Dr. J. C. Evans of Kansas State University, for the use of his unpublished solar model and his help in developing and modifying the computer program used in this study; Dr. K. O. Wright for the tracings and spectrograms, made at the Dominion Astrophysical Observatory, used in this study; and Mr. E. G. Myrick for permission to use certain data from his thesis.

The author acknowledges that the financial support for the use of the computer was provided by the Oklahoma State University Research Foundation.

In addition, I wish to acknowledge the guidance and counseling of my graduate committee, Dr. L. W. Schroeder, Dr. E. E. Kohnke, Dr. D. L. Rutledge, and Dr. R. T. Alciatore, for encouragement and help during my entire graduate education.

Finally, I would like to express appreciation to my wife for the encouragement and understanding during my graduate education. Her encouragement, understanding, and sacrifice has made this investigation possible. To her I owe an eternal debt.

TABLE OF CONTENTS

LIST OF TABLES

LIST OF FIGURES

CHAPTER I

INTRODUCTION

Statement of the Problem

The purpose of this study is to perform a fine atmospheric analysis of the star θ Ursae Majoris employing a detailed model atmosphere computation. A digital computer program which computes a pressure-opacity-flux model for a given temperature distribution and solar abundance was modified and adapted to our investigation. A grid of sixteen model stellar atmospheres with scaled solar-type temperature distributions and with four different values of effective temperatures and surface gravities was computed.

The blanketing and blanketing-free effects for the theoretical UBV colors were computed for each model in order to determine the effect and need for considering line blanketing in calculation of the theoretical colors. The line blanketing effect was computed by multiplying the theoretically computed flux by the absorption factors. The computed values of the UBV colors will be compared to the observed values in order to determine which model of the stellar atmosphere will be selected as the model best describing the star.

The hydrogen line profiles for each model will be computed and compared with Balmer line profiles from tracings made at the Dominion Astrophysical Observatory. The hydrogen line profiles will be used to determine or select a model atmosphere that agrees best with observed values of the star. The model dictated by the hydrogen line profiles will be compared to those dictated by the UBV colors in order to determine if a single model can be selected as representative for θ Ursae Majoris.

CHAPTER II

THE MODEL ATMOSPHERE

Stellar Atmospheres

The atmosphere of a star may be defined as those layers from which a photon, emitted in the outward direction, has a high probability of escaping before it can be absorbed, or, the atmosphere may be defined as those layers of a star directly accessible to observation, in the sense that a detectable amount of radiation which is characteristic of those layers reaches the observer without being absorbed or scattered.

Stellar atmospheres range from 500 to 1,000 km in thickness and the mass of the stellar atmosphere is negligible compared to the mass of the star. Since the radiation we receive from the star was emitted somewhere in the atmosphere of the star, the character of the radiation is determined by the physical conditions in the atmosphere.

Model Stellar Atmospheres

The model atmosphere is the variation of the physical variables--temperature, pressure, electron pressure, density, opacity, and energy flux--as functions of a suitably defined depth variable.

The development of the model atmosphere concept originated in an attempt to explain the details of the emergent intensity from the solar surface and the emergent flux from stars. Certain basic assumptions concering the geometry, equilibrium, and conservation equations, which are consistent with observational evidence, were made in order to reduce the complexity of the model atmosphere.

The spectral distribution of stellar radiation is usually approached on a theoretical basis using the model stellar atmosphere concept. The general problem of representing a real stellar atmosphere by a model is neither mathematically or physically feasible; therefore, several assumptions are made which limit the reality of the model. The theoretical models enable one to calculate properties of the stellar atmosphere, but certain variable parameters must be given before it is possible to construct a model. Once the parameters are specified, the model is used to compute quantities which can be compared with actual stellar observations.

The complexity of the model increases with the number and types of parameters used in the model. Simplifications are introduced in our stellar model, but this forces our model to depart from the real model which is being investigated. This approach is a valid theoretical tool for determining stellar properties and processes because the results of the model atmosphere methods are in good agreement with many observed spectral properties and processes. In order to reduce the complexity of the problem, seven assumptions are made in this study.

Assumptions for the Model Atmosphere

A preliminary fine atmospheric analysis of the star θ Ursae Majoris* was made using a detailed atmospheric computation. The assumptions made

---

*Listed by Johnson and Morgan as a subgiant (spectral type F6, Luminosity class IV). Visual magnitude is 3.3 and its coordinates are $\alpha(1900) = 9^h 26^m$, $\delta(1900) = +52^\circ 8'$ (Keenan and Morgan 1951).

in this investigation are: (i) The star is assumed to be spherically symmetric, non-rotating, and with the linear extent of the atmosphere small compared to the radius. (ii) The atmosphere is assumed to be stratified in homogeneous steady-state, plane parallel layers. (iii) The outer boundary is defined by the condition that no significant quantity of radiation flows into the star across the boundary. (iv) The atmosphere is assumed to contain no significant sources or sinks of energy. (v) The atmosphere is assumed to be in a state of hydrostatic equilibrium under the action of a uniform gravitational field with no radiation, magnetic, or mechanical forces. (vi) The gases are assumed to be in local thermodynamic equilibrium, and (vii) the formation of the line and the continuous spectrum may be treated separately.

The seven assumptions stated will impose certain restrictions on different parameters used in the model. A clarification of some of the assumptions will be stated. Assumption (ii) requires that each layer is defined by a single variable, for instance the geometrical depth, t. Assumption (iv) assumes no significant sources or sinks of energy. Radiative equilibrium is not assumed in this investigation. If we impose the condition of strict radiative equilibrium, we would have been using the classical restricted problem of Milne (Kourganoff 1952). Assumption (v) states that the total pressure at each layer is just the gas pressure. Assumptions (vi) and (vii) concern the nature of the interaction of the gas and radiation fields. Assumption (vi) is equivalent to saying that for each layer the source function for the radiation field is just the Planck function of the local electron temperature. Scattering is neglected and pure absorption is considered as the only mechanism for the formation of the radiation field. Within the region that is responsible for the observed spectrum, it is a reasonable assumption (Bohm 1960; Aller 1963a).

The assumption that the atmosphere is non-magnetic may seem inconsistent. The magnetic forces are not totally neglected because an effective surface gravity was used rather than the dynamical gravity. The magnetic forces produce a magnetic pressure which acts to distend the atmosphere in opposition to the dynamical surface gravity.

The state of the atmosphere is assumed to be one of local thermodynamic equilibrium. At each layer the gas molecules obey Maxwell-Boltzmann statistics so that the ionization and excitation equilibria are determined by the Saha and Boltzmann equations respectively, for the electron kinetic temperature. In local thermodynamic equilibrium the source function, the ratio of the emission coefficient to the absorption coefficient, is the Planck function. Scattering is neglected and pure absorption is assumed to be the only mechanism for the formation of the radiation field.

Temperature Distribution

The temperature is one of the thermodynamic variables that specify the model atmosphere. In thermodynamic equilibrium, the temperature distribution is determined by the energy incident at the bottom of the atmosphere from the deep interior, the mechanism for energy transport, and the sources of continuous absorption. The assumptions that the net flux must be constant at each layer in the atmosphere, the transport mechanisms being either strictly radiative or combined radiative and convective, and the source of continuous opacity, are sufficient to determine the temperature with depth in the atmosphere.

The use of limb-darkening observations together with the energy distribution at the center of the solar disk may be used to determine an empirical temperature distribution for $-1.0 \leq x \leq 0.3$. The depth, x, is equal to the logarithm of the optical depth, τ_o. The subscript "o" denotes the value of the optical depth at $\lambda = 5{,}000$ Angstroms. A comparison of such a temperature distribution with theoretical results indicates a discrepancy. This discrepancy may be related to the blanketing by absorption lines and temperature inhomogenities due to turbulent and convective velocity fields.

An empirical solar temperature distribution by Elste (1955) was used in this study. The scaling of Elste's solar temperature distribution is accomplished in the following manner. Multiply the empirical solar temperatuare at each optical depth, log τ_o, by the ratio of the desired stellar to solar effective temperatures. The solar effective temperature, T_{eff}, was taken to be 5780°K (Aller 1963a). The solar temperature is given at twenty-seven points between the limits of $-4.0 \leq x \leq +1.2$. Table I states the relationships between the solar effective temperature and the scale factors for θ Ursae Majoris using Elste's Model 10. The temperature distributions are given in terms of θ where θ is 5040 divided by the temperature in degrees Kelvin.

The stellar effective temperature is not a true effective temperature because the total integrated flux is not obtained by using this temperature in the Stefan-Boltzmann law. The temperature is an approximation and it will be referred to as the model temperature.

The Pressure-Opacity-Flux Model

The model atmosphere is the variation of the physical variables

TABLE I

SCALED SOLAR TYPE-MODEL FOR θ URSAE MAJORIS

Spectral Type	Elste Model 10	F4	F5	F6	F8
T(eff) ^{o}K	5780	6650	6500	6350	6200
Scale Factor	1.0000	0.8692	0.8892	0.9102	0.9323
Log τ_o			θ(= 5040/T)		
-4.0	1.1431	0.9936	1.0164	1.0404	1.0657
-3.8	1.1425	0.9931	1.0159	1.0399	1.0652
-3.6	1.1414	0.9921	1.0149	1.0389	1.0641
-3.4	1.1398	0.9907	1.0135	1.0374	1.0626
-3.2	1.1379	0.9891	1.0118	1.0357	1.0609
-3.0	1.1350	0.9865	1.0092	1.0331	1.0582
-2.8	1.1310	0.9831	1.0057	1.0294	1.0544
-2.6	1.1250	0.9779	1.0004	1.0240	1.0488
-2.4	1.1180	0.9718	0.9941	1.0176	1.0423
-2.2	1.1070	0.9622	0.9843	1.0076	1.0321
-2.0	1.0930	0.9500	0.9719	0.9948	1.0190
-1.8	1.0760	0.9353	0.9568	0.9794	1.0032
-1.6	1.0560	0.9179	0.9390	0.9612	0.9845
-1.4	1.0340	0.8988	0.9194	0.9411	0.9640
-1.2	1.0090	0.8770	0.8972	0.9184	0.9407
-1.0	0.9820	0.8536	0.8732	0.8938	0.9155
-0.8	0.9520	0.8275	0.8465	0.8665	0.8875
-0.6	0.9180	0.7979	0.8163	0.8356	0.8559
-0.4	0.8790	0.7640	0.7816	9.8001	0.8195
-0.2	0.8340	0.7249	0.7416	0.7591	0.7775
0.0	0.7840	0.6815	0.6971	0.7136	0.7309
0.2	0.7300	0.6345	0.6491	0.6644	0.6806
0.4	0.6750	0.5867	0.6002	0.6144	0.6293
0.6	0.6330	0.5502	0.5629	0.5762	0.5901
0.8	0.6030	0.5241	0.5362	0.5489	0.5622
1.0	0.5840	0.5076	0.5193	0.5316	0.5445
1.2	0.5720	0.4972	0.5086	0.5206	0.5333

as functions of an appropriately defined depth variable. Elste (1955) and Weidmann (1955) discuss the value and convenience of using a logarithmic optical depth scale rather than the actual physical depth because of the relationship between the two. The logarithmic optical depth scale is approximately linearly proportional to the physical depth making it a more desirable variable to use than the optical depth.

The logarithm of the continuum optical depth is related to the physical depth scale t by the relation

$$x = \log \tau_o = \log \int_o^t \frac{\kappa_o(t)}{m_o \sum_i \varepsilon_i \mu_i} \rho(t)\, dt \quad , \qquad (2\text{-}1)$$

where $\kappa_o(t)$ = the continuous absorption coefficient per hydrogen particle at 5000 Angstroms,

m_o = the mass in grams of a unit atomic weight,

μ_i = the atomic weight of species i,

$\varepsilon_i = n_i/n_H$ = the number abundance of element i relative to hydrogen,

$\rho(t)$ = the density of stellar material.

The reciprocal of $m_o \sum_i \varepsilon_i \mu_i$ is the number of hydrogen particles per gram of material.

The atmosphere was divided into twenty-seven layers extending from -4.0 to + 1.2 in the logarithm of the optical depth. The corresponding geometrical depth at each layer of the atmosphere may be calculated by inverting and solving Equation (2-1) and assigning a geometrical depth of zero at an optical depth of 0.01

Ionization Equilibrium

We assumed the atmosphere to be one in local thermodynamic equilibrium. This assumption implies that the gas particles obey the Maxwell-Boltzmann statistics so that the Boltzmann and Saha equations are valid. If we assume only neutral and singly ionized constituents and neglect helium ionization and all molecules, the Saha equation and the perfect gas law determine the contribution of various species to the total gas pressure and the electron pressure. Programs have been developed assuming the ionization of helium, but the effect of the ionization of helium is negligible over the temperature range covered in this study.

The Saha equation for the ratio of single ions to neutral particles of species i is given by (Aller 1963a)

$$\frac{n_1}{n_o} = 10^{\log(u_1/u_0) + (9.0801 - 2.5 \log \theta - \log P_e) - \chi_o \theta} \equiv \frac{\Phi_i}{P_e}, \qquad (2\text{-}2)$$

where $u_r(\theta)$ = the partition function of the rth ionization stage,

θ = the reciprocal of the temperature. $\theta = 5040/T^o(K)$,

P_e = the electron pressure,

χ_r = the ionization potential between the rth and (r + 1)st ionization stages in electron volts,

n_1 = the number density of singly ionized particles of species i,

n_o = the number density of neutral particles of species i,

Φ_i/P_e = the Saha equation for the ratio of single ions to neutral particles of species i.

The degree of ionization--the ratio of the number density of ions to atoms and ions--is given by

$$\left(\frac{n_1}{n_o + n_1}\right)_i = \frac{\Phi_i/P_e}{1 + \Phi_i/P_e} \equiv Xi\ . \qquad (2\text{-}3)$$

If we neglect helium ionization, molecular dissociation, and negative ions, and assume one ionization stage, the number density of free electrons due to the ionization of a particular species is equal to the number density of ions of that species. The ratio of all atoms, ions, and electrons to electrons is

$$\frac{n}{n_e} = \frac{n_{He} + \sum_i (n_o + n_i + n_e)_i}{\sum_i (n_e)_i}, \tag{2-4}$$

where n_{He} = the helium number density. Dividing the numerator and denominator of Equation (2-4) by the number of hydrogen particles, n_H, introducing ε_i, and use the perfect gas law to convert to a ratio of pressure, Equation (2-4) becomes

$$\frac{P_g}{P_e^{\,2}} = \frac{\sum_i \varepsilon_i (1 + Xi)}{P_e \sum_i \varepsilon_i Xi}. \tag{2-5}$$

The reason for dividing both sides of Equation (2-5) by P_e is $P_g/P_e^{\,2}$ is less sensitive to P_e than to θ (Weidemann 1955) which is important in the actual computations.

Gas Pressure

The equation for hydrostatic equilibrium can be written in terms of the continuous absorption coefficient at 5000 Å, the effective surface gravity, and a conversion to a logarithm optical depth scale. This form of the equation is

$$dP_g = \frac{g m_o \sum_i \varepsilon_i \mu_i}{\kappa_o} \left(\frac{\tau_o}{\mathrm{Mod}}\right) dx, \tag{2-6}$$

where g = the effective surface gravity,

$$\text{Mod} = \log_{10} e = 0.43429.$$

Multiplying Equation (2-6) by $P^{1/2}$ and integrating from the outer boundary or the top of the atmosphere, where $P_g = 0$, to the depth x, an expression for the gas pressure at the point x is obtained (Evans 1966). In logarithmic form the equation is

$$\log P_g = \frac{2}{3} \log \left(\frac{3}{2} \frac{\kappa}{\text{Mod}}\right) + \frac{2}{3} \log \int_{-\infty}^{x} \sqrt{\frac{P_g}{P_e^2}} \frac{\tau_o}{(\kappa_o/P_e)} dx' , \qquad (2\text{-}7)$$

where $\kappa = m_o g \Sigma \varepsilon_i \mu_i$.

The pressure model computation is an iteration on the electron pressure which can be obtained by the relation (Evans 1966)

$$\log P_e = \tfrac{1}{2} \left[\log P_g - \log P_g/P_e^2\right]. \qquad (2\text{-}8)$$

The density in each layer can be computed using the perfect gas law written in logarithmic form by the relation

$$\log P = \log P_g = \log (m_o \Sigma \varepsilon_i \mu_i) - \log k - \log (5040/\theta), \qquad (2\text{-}9)$$

where k = the Boltzmann constant.

The Sources of Continuous Absorption

The major assumptions involved in the calculations of the continuous absorption coefficient are: (a) the neglect of all molecular absorption except H_2^+; (b) the neglect of all negative ion absorption except H^-; and (c) the use of a hydrogenic approximation for metal absorption. The total absorption coefficient κ_λ includes, in order of importance, bound-free (bf) and free-free (ff) absorption due to H^-, H, H_2^+, and a total absorption coefficient for all metals (Evans 1966, Elste 1965).

The metal absorption coefficient was integrated over the ionization continuum rather than summing to obtain a smooth curve. In addition, the total absorption coefficient is multiplied by a correction term for stimulated emission of radiation and this product has added to it a scattering coefficient for Rayleigh scattering by neutral hydrogen and Thompson scattering by free electrons. The total monochromatic absorption coefficient per hydrogen particle per unit electron pressure at any depth in the atmosphere can be written in the form

$$\frac{\kappa_\lambda}{P_e} = \frac{\kappa_\lambda(H_{bf,ff})}{P_e} + \frac{\kappa_\lambda(H^-_{bf})}{P_e} + \frac{\kappa_\lambda(H^-_{ff})}{P_e} + \frac{\kappa_\lambda(H_2^+ bf,ff)}{P_2} + \qquad (2\text{-}10)$$

$$\frac{\kappa_\lambda(\text{Metals}_{bf,ff})}{P_e}\left(1 - e^{-\frac{hc}{\lambda kT}}\right) + \frac{\sigma(H,e^-)}{P_e} \; .$$

The Atomic Data

The adopted chemical composition used to compute the ionization equilibrium and the continuous absorption is made up of hydrogen, helium and a number of metals. The effect of several metals of similar ionization potential can be obtained by grouping them together in one abundance and using the ionization potential of the most abundant of the group. This has been done in Table II where the secondary elements are shown in parentheses. The relative abundance by number is taken from Goldberg, Müller and Aller (1960) for the sun. The abundance for helium is estimated from other investigations. The necessary atomic quantities such as partition functions, atomic weights, ionization potentials, et cetera, used in the calculations have been tabulated by Evans (1966).

TABLE II

ADOPTED ATMOSPHERIC ABUNDANCE FOR THE MODEL COMPUTATIONS

Element	log ε	Element	log ε
H(O,N)	0.004	K	-7.300
He	-0.824	Ca	-6.120
C(S,P)	-3.116	Cr(Ti,V)	-6.910
Na	-5.700	Fe(Co,Cu)	-5.570
Mg	-4.600	Ni(Mn)	-6.090
Si	-4.500		

Surface Flux

Aller (1963a) gives the solution to the equation of radiative transfer for the surface flux. A transfer equation can be written for the monochromatic radiant intensity from whose solution an integral equation may be derived for the emergent flux (Kourganoff 1952):

$$F_\lambda(0) = 2\int_0^\infty S_\lambda(\tau_\lambda)E_2(\tau_\lambda)d\tau_\lambda, \qquad (2\text{-}11)$$

where the optical depth at the wavelength λ is given by

$$\tau_\lambda(x) = \int_{-\infty}^{t} \frac{\kappa_\lambda(t)}{\kappa_o(t)}\left(\frac{\tau_o}{\text{Mod}}\right)dt, \qquad (2\text{-}12)$$

where S_λ = the source function which is the Planck function,

E = the second exponential-integral function given by

$$E_2 = \int_{-\infty}^{t} \frac{e^{-\frac{t\omega}{2}}}{\omega^2}\, d\omega\ . \qquad (2\text{-}13)$$

The actual flux is given by $\pi F_\lambda(0)$.

Computational Procedures

The computer program was developed by Elste and later modified by

Evans (1969). The input parameters used in the computations are: (i) effective surface gravity; (ii) the temperature distribution; (iii) chemical composition; (iv) an initial estimate of the electron pressure. Using the initial electron pressure, the value of $P_g/P_e^{\,2}$ is calculated from Equation (2-5). The temperature distribution and initial electron pressure are used in Equation (2-10) to determine κ_o/P_e where κ_o represents the continuous absorption coefficient at λ 5000. The value of κ_o/P_e, the chemical composition, the logarithm of the effective surface gravity, and previously computed quantity $P_g/P_e^{\,2}$ are used in Equation (2-7) to calculate an initial estimate of the gas pressure P_g. Using Equation (2-8), log P_g, and $P_g/P_e^{\,2}$ are used to compute a new estimate for the electron pressure. This procedure is then repeated until it converges to a consistent value for the electron pressure. In practice the convergence does not depend strongly on the initial electron pressure since $P_g/P_e^{\,2}$ and κ_o/P_e are stronger functions of temperature than electron pressure. For the opacity model, the absorption coefficient for wavelengths other than 5000 angstroms is computed from Equation (2-10) and optical depth for these wavelengths is computed by integrating Equation (2-12). The emitted flux is obtained from the same wavelengths as the opacity model by integrating Equation (2-11). The opacity flux model was computed for the interval $\lambda\lambda$2,000 - 21,000 with twenty-seven values between 2,000 and 10,000 angstroms and one each for 15,000 and 21,000 angstroms.

This method of computation is desirable for the range of temperatures encountered in the A5 to G5 stars because of the rapid convergence and the relative insensitivity to the initial estimate of P_e.

The computational procedure will give a table of the variation of the thermodynamic parameters with the depth x and a table relating the different optical depth scales as a function of x. In addition, this information will be used as part of the data input for the hydrogen line programs.

The Computed Models

A grid of sixteen stellar model atmospheres with scaled solar type (Elste Model 10) temperature distributions was computed for a range of effective temperatures ($6200^{\circ}K \le T_{eff} \le 6650^{\circ}K$), surface gravities ($3.8 \le \log g \le 4.4$) and the solar abundance. A representative model atmosphere is listed in Table III for which $T_{eff} = 6500^{\circ}K$ and $\log g = 4.2$. "B", the helium to hydrogen number density ratio, was set at 0.1250. This value is somewhat less than that indicated by Table II since we are concerned with stars of earlier spectral type (and, therefore, presumably younger) than the sun. From Table II a value of 3.2306 was assigned for "A", where $A = \log n_H/\Sigma n$ metals.

TABLE III

REPRESENTATIVE MODEL ATMOSPHERE

SOLAR TYPE MODEL (ELSTE MODEL 10) F5 V

T(EFF) = 6500.00 LOG G = 4.2000 B = 0.1250 A = 3.2306 NO. ITERATIONS = 5

LOG TAU (5000)	THETA MODEL	TEMP. (K)	LOG PE	LOG PG	LOG K/PE (5000)	MEAN MOL. WT.	LOG DENSITY	TURBULENCE (KM/SEC)
-4.00	1.0164	4959.	-0.9655	2.8943	-25.0394	1.3597	-8.5874	0.0
-3.80	1.0159	4961.	-0.9217	2.9590	-25.0458	1.3597	-8.5230	0.0
-3.60	1.0149	4966.	-0.8340	3.0884	-25.0573	1.3597	-8.3940	0.0
-3.40	1.0135	4973.	-0.7437	3.2159	-25.0681	1.3597	-8.2671	0.0
-3.20	1.0118	4981.	-0.6518	3.3414	-25.0783	1.3597	-8.1423	0.0
-3.00	1.0092	4994.	-0.5559	3.4647	-25.0891	1.3597	-8.0202	0.0
-2.80	1.0057	5011.	-0.4568	3.5856	-25.1006	1.3597	-7.9008	0.0
-2.60	1.0004	5038.	-0.3514	3.7039	-25.1144	1.3597	-7.7848	0.0
-2.40	0.9941	5070.	-0.2436	3.8198	-25.1294	1.3597	-7.6716	0.0
-2.20	0.9843	5120.	-0.1233	3.9329	-25.1500	1.3597	-7.5628	0.0
-2.00	0.9719	5186.	0.0062	4.0425	-25.1747	1.3597	-7.4587	0.0
-1.80	0.9568	5268.	0.1466	4.1482	-25.2038	1.3597	-7.3598	0.0
-1.60	0.9390	5367.	0.3001	4.2494	-25.2374	1.3597	-7.2668	0.0
-1.40	0.9194	5482.	0.4645	4.3455	-25.2743	1.3597	-7.1798	0.0
-1.20	0.8972	5617.	0.6457	4.4359	-25.3159	1.3596	-7.1000	0.0
-1.00	0.8732	5772.	0.8409	4.5199	-25.3611	1.3596	-7.0278	0.0
-0.80	0.8465	5954.	1.0564	4.5970	-25.4119	1.3595	-6.9643	0.0
-0.60	0.8163	6174.	1.2982	4.6661	-25.4700	1.3593	-6.9110	0.0
-0.40	0.7816	6448.	1.5738	4.7263	-25.5373	1.3589	-6.8698	0.0
-0.20	0.7416	6796.	1.8892	4.7766	-25.6145	1.3581	-6.8425	0.0
0.0	0.6971	7230.	2.2382	4.8168	-25.6974	1.3563	-6.8298	0.0
0.20	0.6491	7765.	2.6131	4.8476	-25.7767	1.3519	-6.8314	0.0
0.40	0.6002	8397.	2.9934	4.8701	-25.8342	1.3418	-6.8462	0.0
0.60	0.5629	8954.	3.2834	4.8870	-25.8516	1.3260	-6.8623	0.0
0.80	0.5362	9399.	3.4912	4.9017	-25.8460	1.3070	-6.8749	0.0
1.00	0.5193	9705.	3.6244	4.9167	-25.8352	1.2905	-6.8794	0.0
1.20	0.5086	9910.	3.7088	4.9262	-25.8253	1.2777	-6.8833	0.0

CHAPTER III

THE THEORETICAL UBV COLORS

The UBV System

In modern work all magnitude and color standards are calibrated by photoelectric photometry because of the greater accuracy achieved by this method. Several color systems have been developed and used for special cases, but different systems have advantages and disadvantages. One of the most widely used color systems is the UBV three-color photometry system.

The UBV system (U = ultraviolet, B = blue, and V = visual) developed by Johnson and Morgan (1953) is a three-color system which has proved extremely useful for work on problems of stellar evolution and galactic structure. It employs an RCA type 1P21 multiplier phototube with appropriate filters. The Johnson-Morgan system has a number of important advantages in that it reduces difficulties caused by the Balmer jump in the older magnitudes, includes stars of all luminosity and spectral classes well distributed over the sky, and permits one to assess the effects and amount of space reddening.

Some of the values assigned to the UBV system are (i) the approximate effective wavelengths of U, B, and V are, respectively 3500, 4350, and 5500 angstroms; (ii) the V magnitudes are very close to the old visual magnitudes and may be regarded as essentially equivalent to them, but the B magnitudes differ from the international photographic magnitudes because they do not include the Balmer limit; (iii) the zero points of the B and U magnitudes are fixed by the requirement that the U-B and B-V color indices are both equal to zero for the mean of six bright stars of spectral class AO V.

If appropriate sensitivity and optical transmissivity curves for the UBV magnitude systems were known it would be possible to correctly predict stellar colors from energy scans. Such a procedure has not proven possible and the UBV system must be regarded as empirically defined in terms of measurements made on certain standard stars. The failure may be in the energy distribution, uncertainties in the basic response curves of the photoelectric cell, filter, and telescope. Stellar colors are often available when energy distributions are not and we must use colors to obtain checks on stellar temperatures.

It must be emphasized that the UBV magnitudes of a star depend not only on its intrinsic luminosity and surface temperature, but also on its chemical composition and the role of chemical composition must be kept in mind particularly when dealing with stars of abnormal H/metal ratios.

Some general principals that should be used in designing any color system are as follows. (i) The larger the number of colors, the narrower will be the bandwidths, resulting in a smaller response per band. (ii) The bands should be spaced as widely as possible in order to preserve the ability of color index to indicate physical parameters. (iii) Design a color system, if possible, to match a standard color system of known magnitudes and colors for a large variety of stars.

Matsushima-Hall Method

Matsushima and Hall (1969) investigated the magnitude of the correction required by the new calibration for the transformation formula used by Mihalas (1966) to normalize the theoretical colors to the Johnson-Morgan UBV system. The transformation relation used by Mihalas was derived by Matthews and Sandage (1963) on the basis of the energy spectra of seven stars measured on the old photometric calibration.

Matsushima and Hall assumed the observed colors, B-V or U-B, to have a linear relation with the unnormalized theoretical colors, b-v or u-b, such that

$$B\text{-}V = A(b\text{-}v) + B, \tag{3-1}$$

where

$$b\text{-}v = 2.5 \log \int_0^\infty F_\lambda S_v(\lambda) d_\lambda - 2.5 \log \int_0^\infty F_\lambda S_b(\lambda) d\lambda, \tag{3-2}$$

F_λ is the flux per unit wavelength at wavelength λ,

S_v and S_b represent the response function of the V and B filter-photometer systems,

A and B are constants to be determined by an empirical fit between the observed colors and the colors computed from Equation (3-2).

The S functions are tabulated by Matthews and Sandage. A numerical integration of Equation (3-2) was performed in order to examine possible descrepancies that may exist. The most important fact determined from the integration of Equation (3-2) was that an effective temperature was obtained which was approximately ten to twenty per cent greater than the values determined by Mihalas.

The Matsushima-Hall and Matthews-Sandage computations do not take into account the flux removed by absorption lines. They expect that the blocking of energy by hydrogen lines will be large, while metal lines should be very weak in their spectra. They suggest a reasonable estimate of the magnitude of the energy removed by hydrogen lines may be made by taking the difference between theoretical colors computed with and without the lines from a model closely representing the star. The correction for hydrogen lines gives a transformation similar to those given by Matthews and Sandage. A method of least square fits of the stars excluding those of luminosity classes other than the main sequence, yields

$$U-B = 0.896\ (u-b) - 1.288, \qquad (3\text{-}3)$$

$$B-V = 0.982\ (b-v) + 0.791. \qquad (3\text{-}4)$$

The validity of the transformations given by Equations (3-3) and (3-4) may be limited because they do not include line blanketing effects and the basic data include only blue stars.

Equations (3-3) and (3-4) are similar to the equations derived by Matthews and Sandage in both the color dependency and the constant term. The difference in theoretical colors obtained from the two transformation relations differ by 0.01 to 0.02 magnitudes. This close agreement is expected since neither method allowed any correction for line blocking in the derivations of the equations. An error in the estimation of the hydrogen content could change the U-B relation by a significant amount, while the corresponding change for B-V may be negligible.

Matthews and Sandage Method

It is possible, and many times desirable, to compute the UBV colors of radiant sources with given energy distribution. The computation can be performed once the transmission functions, S(λ), of the U,B,V system are known. Melbourne (1960) showed that the S(λ) functions tabulated by Johnson will not predict exactly the U-B and B-V colors for real stars of known energy distribution unless a systematic zero-point correction of -0.13 is applied to the computed natural b-v magnitude and +0.17 is added to the computed u-b magnitude before applying Johnson's (1953) empirically determined transformation equation. These corrections assume that there is no color equation between the theoretical colors based on S(λ) and the U-B and B-V values adapted for standard stars in the sky.

Matthews and Sandage (1963) confirm Melbourne's zero point procedure for B-V colors. They derive equations that can be used to convert theoretical calculations based on the adopted S(λ) to the empirical U,B,V system. Predicted U-B and B-V colors for any arbitrary flux distribution function F(λ) can be obtained also. The transmission functions used by Matthews and Sandage were taken from Melbourne's thesis. Table IV lists the transmission functions from Melbourne's thesis and these transmission functions are used in this study to compute the U-B and B-V colors. A complete derivation and explanation of the equations are given by Matthews and Sandage (1963).

The procedure used by Matthews and Sandage for computing the U-B and B-V colors for any arbitrary energy distribution F(λ) was done in the following manner. (i) Use the S(λ) functions of Table IV and Equations (3-5) and (3-6) to compute the colors u-b and b-v.

TABLE IV

ADOPTED TRANSMISSION FUNCTIONS AFTER MELBOURNE AND CODE

λ	S(λ)		
Å	u	b	v
3000	0.025		
3100	0.250		
3200	0.680		
3300	1.137		
3400	1.650		
3500	2.006	0.000	
3600	2.250	0.006	
3700	2.337	0.080	
3800	1.925	0.337	
3900	0.650	1.425	
4000	0.197	2.253	
4100	0.070	2.806	
4200	0.000	2.950	
4300		3.000	
4400		2.937	
4500		2.780	
4600		2.520	
4700		2.230	
4800		1.881	0.020
4900		1.550	0.175
5000		1.275	0.900
5100		0.975	1.880
5200		0.695	2.512
5300		0.430	2.850
5400		0.210	2.820
5500		0.055	2.625
5600		0.000	2.370
5700			2.050
5800			1.720
5900			1.413
6000			1.068
6100			0.795
6200			0.567
6300			0.387
6400			0.250
6500			0.160
6600			0.110
6700			0.081
6800			0.061
6900			0.045
7000			0.028
7100			0.017
7200			0.007

$$u\text{-}b = 2.5 \log \frac{\int_0^\infty S_b (\lambda)F(\lambda)d_\lambda}{\int_0^\infty S_u (\lambda)F(\lambda)d_\lambda} . \quad (3\text{-}5)$$

$$b\text{-}v = 2.5 \log \frac{\int_0^\infty S_v (\lambda)F(\lambda)d_\lambda}{\int_0^\infty S_b (\lambda)F(\lambda)d_\lambda} . \quad (3\text{-}6)$$

(ii) Use Equations (3-7) and (3-8) to compute the U-B and B-V colors.

$$U\text{-}B = 0.921 (u\text{-}b) - 1.308. \quad (3\text{-}7)$$

$$B\text{-}V = 1.024 (b\text{-}v) + 0.81. \quad (3\text{-}8)$$

Theoretical Colors Without Line Blanketing

The model atmosphere program was designed to compute the flux distribution function, F(λ), for twenty-two different wavelengths between λ2000 and λ7460. Four different values of log g and four different values of effective temperature, indicative of four different spectral types, were considered, resulting in a grid of sixteen model atmospheres. In order to use the adopted transmission functions, S(λ), given by Matthews and Sandage (1963), the values of F(λ) must be known at each one hundred angstroms over the interval under investigation. F(λ) was plotted as a function of wavelength using the values computed from the atmosphere program and a smooth curve was drawn through the plotted points in order that the values of F(λ) might be read at the desired intervals. Table V gives the values of $F(\lambda) \times 10^{-5}$ and $\log F(\lambda) \times 10^{-8}$ rather than the values obtained from the computer program. Figure 1 illustrates the variation of the computed flux for a solar-type star over the interval λλ3000-7200.

The transmission functions were then multiplied by the appropriate

TABLE V

THEORETICAL FLUX DISTRIBUTIONS

Spectral Type	T_{eff} ^oK	log g	λ	F(λ) x 10^{-5}	log F(λ) - 8
F4 V	6650	3.8	2000.00	00.72	4.8569
			2500.00	26.92	6.4300
			3000.00	43.65	6.6402
			3200.00	44.88	6.6521
			3400.00	45.61	6.6591
			3645.00	45.50	6.6580
			3650.00	76.10	6.8814
			3889.05	76.35	6.8828
			4000.00	74.75	6.8736
			4104.74	74.56	6.8725
			4200.00	73.25	6.8648
			4340.47	70.37	6.8474
			4600.00	65.65	6.8172
			4861.33	60.58	6.7823
			5150.00	56.48	6.7519
			5383.37	53.16	6.7256
			5560.00	50.41	6.7025
			5895.92	45.90	6.6618
			6050.00	43.78	6.6413
			6562.82	37.79	6.5774
			7000.00	33.21	6.5213
			7460.00	29.14	6.4645
F4 V	6650	4.0	2000.00	00.73	4.8606
			2500.00	28.19	6.4501
			3000.00	45.67	6.6596
			3200.00	46.75	6.6698
			3400.00	47.38	6.6756
			3645.00	47.10	6.6730
			3650.00	75.91	6.6730
			3889.05	76.21	6.8820
			4000.00	74.61	6.8728
			4101.47	74.46	6.8719
			4200.00	73.17	6.8643
			4340.47	70.31	6.8470
			4600.00	65.60	6.8169
			4861.33	60.56	6.7822
			5150.00	56.49	6.7520
			5385.37	53.17	6.7257
			5560.00	50.44	6.7028
			5895.92	45,94	6.6622
			6050.00	43.82	6.6417
			6562.82	37.84	6.5779
			7000.00	33.26	6.5219
			7460.00	29.19	6.4652

TABLE V (Continued)

Spectral Type	T_{eff} °K	log g	λ	F(λ) x 10^{-5}	log F(λ) $-^{8}$
F4 V	6650	4.2	2000.00	00.73	4.8649
			2500.00	11.10	6.0419
			3000.00	47.66	6.6782
			3200.00	48.63	6.6869
			3400.00	49.16	6.6915
			3645.00	48.70	6.6875
			3650.00	75.72	6.8792
			3889.05	76.07	6.8812
			4000.00	74.51	6.8722
			4104.74	74.35	6.8713
			4200.00	73.08	6.8638
			4340.47	70.25	6.8466
			4600.00	65.57	6.8167
			4861.33	60.55	6.7821
			5150.00	56.51	6.7521
			5385.37	53.20	6.7259
			5560.00	50.47	6.7030
			5895.92	45.97	6.6625
			6050.00	43.87	6.6421
			6562.82	37.88	6.5784
			7000.00	33.30	6.5224
			7460.00	29.23	4.6580
F4 V	6650	4.4	2000.00	00.74	4.8701
			2500.00	30.71	6.4872
			3000.00	49.66	6.6960
			3200.00	50.50	6.7033
			3400.00	50.91	6.7068
			3645.00	50.28	6.7014
			3650.00	75.58	6.8784
			3889.05	75.78	6.8806
			4000.00	74.41	6.8716
			4104.74	74.27	6.8708
			4200.00	73.01	6.8634
			4340.47	70.25	6.8463
			4600.00	65.55	6.8166
			4861.33	60.53	6.7820
			5150.00	56.51	6.7521
			5385.37	53.21	6.7260
			5560.00	50.48	6.7031
			5895.92	46.00	6.6628
			6050.00	43.88	6.6423
			6562.82	37.91	6.5788
			7000.00	33.33	6.5228
			7460.00	29.27	6.4664
F5 V	6500	3.8	2000.00	00.43	4.6339
			2500.00	22.38	6.3499

TABLE V (Continued)

Spectral Type	T_{eff} ^oK	log g	λ	$F(\lambda) \times 10^{-5}$	$\log F(\lambda)^{-8}$
F5 V	6500	3.8	3000.00	39.85	6.6004
			3200.00	41.13	6.6142
			3400.00	42.00	6.6232
			3645.00	42.03	6.6236
			3650.00	66.44	6.8224
			3889.05	67.53	6.8295
			4000.00	66.41	6.8222
			4101.74	66.56	6.8232
			4200.00	65.55	6.8166
			4340.47	63.18	6.8006
			4600.00	59.27	6.7728
			4861.33	55.00	6.7404
			5150.00	51.52	6.7120
			5383.37	48.67	6.6873
			5560.00	46.28	6.6654
			5895.92	42.33	6.6267
			6050.00	40.46	6.6070
			6562.82	35.12	6.5455
			7000.00	30.98	6.4911
			7460.00	27.30	6.4361
F5 V	6500	4.0	2000.00	00.43	4.6372
			2500.00	23.39	6.3690
			3000.00	41.60	6.6191
			3200.00	42.78	6.6312
			3400.00	43.54	6.6389
			3645.00	43.43	6.6378
			3650.00	66.33	6.8217
		5	3889.05	67.46	6.8290
			4000.00	66.34	6.8218
			4104.74	66.48	6.8227
			4200.00	65.51	6.8163
			4340.47	63.10	6.8004
			4600.00	59.24	6.7726
			4861.33	54.99	6.7403
			5150.00	51.52	6.7120
			5358.37	48.70	6.6875
			5560.00	46.29	6.6655
			5898.92	42.35	6.6269
			6050.00	40.43	6.6072
			6562.82	35.15	6.5459
			7000.00	31.02	6.4916
			7460.00	27.33	6.4366
F5 V	6500	4.2	2000.00	00.44	4.6414
			2500.00	24.38	6.3870
			3000.00	43.33	6.6368
			3200.00	44.41	6.6475

TABLE V (Continued)

Spectral Type	T_{eff} °K	log g	λ	F(λ) x 10^{-5}	log F(λ)-^{8}
F5 V	6500	4.2	3400.00	45.08	6.6540
			3645.00	44.82	6.6515
			3650.00	66.24	6.8211
			3889.05	67.39	6.8286
			4000.00	66.28	6.8160
			4104.74	66.44	6.8224
			4200.00	65.46	6.8160
			4340.47	63.11	6.8001
			4600.00	59.22	6.7725
			4861.33	54.98	6.7402
			5150.00	51.52	6.7120
			5385.37	48.71	6.6876
			5560.00	46.30	6.6656
			5895.92	42.37	6.6271
			6050.00	40.49	6.6074
			6562.82	35.17	6.5462
			7000.00	31.04	6.4919
			7460.00	27.36	6.4371
F5 V	6500	4.4	2000.00	00.44	4.6465
			2500.00	25.35	6.4039
			3000.00	45.06	6.6538
			3200.00	46.04	6.6631
			3400.00	46.61	6.6685
			3645.00	46.20	6.6646
			3650.00	66.18	6.8207
			3889.05	67.34	6.8283
			4000.00	66.24	6.8211
			4104.74	66.39	6.8221
			4200.00	65.42	6.8157
			4340.47	63.08	6.7999
			4600.00	59.21	6.7724
			4861.33	54.98	6.7402
			5150.00	51.54	6.7121
			5385.37	48.71	6.6876
			5560.00	46.31	6.6657
			5895.92	42.39	6.6273
			6050.00	40.51	6.6076
			6562.82	35.19	6.5464
			7000.00	31.06	6.4922
			7460.00	27.38	6.4374
F6 V	6350	3.8	2000.00	00.27	4.4163
			2500.00	18.80	6.2572
			3000.00	36.00	6.5566
			3200.00	37.37	6.5725
			3400.00	38.34	6.5836
			3645.00	38.52	6.5857

TABLE V (Continued)

Spectral Type	T_{eff} ^oK	log g	λ	F(λ) x 10^{-5}	log F(λ)-^{8}
F6 V	6350	3.8	3650.00	57.65	6.7608
			3889.05	59.44	6.7741
			4000.00	58.72	6.7688
			4104.74	59.13	6.7718
			4200.00	58.28	6.7665
			4340.47	56.48	6.7519
			4600.00	53.26	6.7264
			4861.33	49.72	6.6965
			5150.00	46.78	6.6700
			5385.37	44.38	6.6472
			5560.00	42.30	6.6263
			5895.92	38.88	6.5897
			6050.00	37.21	6.5707
			6562.82	32.49	6.5118
			7000.00	28.79	6.4593
			7460.00	25.47	6.4060
F6 V	6360	4.0	2000.00	00.27	4.4196
			2500.00	18.85	6.2753
			3000.00	37.53	6.5744
			3200.00	38.80	6.5888
			3400.00	39.68	6.5986
			3645.00	39.73	6.5991
			3650.00	57.62	6.7606
			3889.05	59.42	6.7739
			4000.00	58.70	6.7686
			4104.74	59.10	6.7716
			4200.00	58.39	6.7663
			4340.47	56.46	6.7517
			4600.00	53.25	6.7263
			4861.33	49.72	6.6965
			5150.00	46.77	6.6700
			5385.37	44.39	6.6473
			5560.00	42.31	6.6264
			5895.92	38.89	6.5898
			6050.00	37.23	6.5709
			6562.82	32.51	6.5120
			7000.00	28.82	6.4596
			7460.00	25.49	6.4063
F6 V	6350	4.2	2000.00	00.27	4.4240
			2500.00	19.61	6.2922
			3000.00	39.30	6.5914
			3200.00	39.85	6.6042
			3400.00	40.77	6.6128
			3645.00	40.93	6.6120
			3650.00	57.61	6.7605
			3889.05	59.40	6.7738

TABLE V (Continued)

Spectral Type	T_{eff} °K	log g	λ	F(λ) x 10^{-5}	log F(λ)-^{8}
F6 V	6350	4.2	4000.00	58.68	6.7685
			4101.74	59.08	6.7714
			4200.00	58.42	6.7662
			4340.47	56.44	6.7516
			4600.00	53.25	6.7263
			4861.33	49.72	6.6964
			5150.00	46.79	6.6701
			5385.37	44.39	6.6473
			5560.00	42.31	6.6264
			5895.92	38.81	6.5889
			6050.00	37.24	6.5710
			6562.82	32.45	6.5112
			7000.00	28.83	6.4598
			7460.00	25.51	6.4066
F6 V	6350	4.4	2000.00	00.27	4.4297
			2500.00	20.34	6.3082
			3000.00	40.50	6.6074
			3200.00	41.58	6.6189
			3400.00	42.31	6.6264
			3645.00	42.09	6.6242
			3650.00	57.61	6.7605
			3889.05	59.40	6.7738
			4000.00	58.73	6.7684
			4101.74	59.06	6.7713
			4200.00	58.36	6.7661
			4340.47	56.43	6.7515
			4600.00	53.24	6.7262
			4861.33	49.71	6.6964
			5150.00	46.79	6.6701
			5383.37	44.39	6.6473
			5560.00	42.32	6.6265
			5895.92	38.91	6.5900
			6050.00	37.25	6.5711
			6562.82	32.53	6.5123
			7000.00	28.84	6.4599
			7560.00	25.52	6.4069
F8 V	6200	3.8	2000.00	00.16	4.2029
			2500.00	14.11	6.1496
			3000.00	32.22	6.5081
			3200.00	33.61	6.5265
			3400.00	34.67	6.5399
			3645.00	34.99	6.5439
			3650.00	49.72	6.6965
			3889.05	52.04	6.7163
			4000.00	51.66	6.7131
			4101.74	52.28	6.7183
			4200.00	51.78	6.7142

TABLE V (Continued)

Spectral Type	T_{eff} ^oK	log g	λ	F(λ) x 10^{-5}	log F(λ)-8
F8 V	6200	3.8	4340.47	50.23	6.7010
			4600.00	47.63	6.6779
			4861.33	44.72	6.6505
			5150.00	42.27	6.6260
			5385.37	40.27	6.6050
			5560.00	38.48	6.5852
			5895.92	35.54	6.5507
			6050.00	34.09	6.5326
			6562.82	29.94	6.4762
			7000.00	26.64	6.4256
			7460.00	23.67	6.3742
F8 V	6200	4.0	2000.00	00.17	4.2066
			2500.00	14.70	6.1666
			3000.00	33.50	6.5251
			3200.00	34.83	6.5419
			3400.00	35.81	6.5540
			3645.00	36.02	6.5565
			3650.00	49.75	6.6968
			3889.05	52.06	6.7165
			4000.00	51.67	6.7132
			4101.47	52.28	6.7183
			4200.00	51.78	6.7142
			4340.47	50.23	6.7010
			4600.00	47.62	6.6779
			4861.33	44.72	6.6505
			5150.00	42.27	6.6260
			5385.37	40.37	6.6050
			5560.00	38.51	6.5852
			5895.92	35.54	6.5507
			6050.00	34.09	6.5326
			6562.82	29.94	6.4763
			7000.00	26.66	6.4258
			7460.00	23.67	6.3743
F8 V	6200	4.2	2000.00	00.16	4.2117
			2500.00	15.23	6.1828
			3000.00	34.79	6.5414
			3200.00	36.03	6.5566
			3400.00	36.94	6.5675
			3645.00	37.03	6.5686
			3650.00	49.81	6.6973
			3889.05	52.08	6.7167
			4000.00	51.69	6.7134
			4101.74	52.29	6.7184
			4200.00	51.80	6.7143
			4340.47	50.24	6.7011
			4600.00	47.64	6.6780

TABLE V (Concluded)

Spectral Type	T_{eff} ^oK	log g	λ	F(λ) x 10^{-5}	log F(λ)-8
F8 V	6200	4.2	4861.33	44.73	6.6506
			5150.00	42.28	6.6261
			5385.37	40.28	6.6051
			5560.00	38.49	6.5853
			5895.92	35.55	6.5509
			6050.00	34.09	6.5327
			6562.82	29.96	6.4765
			7000.00	26.66	6.4259
			7460.00	23.69	6.3746
F8 V	6200	4.4	2000.00	00.17	4.2183
			2500.00	15.76	6.1976
			3000.00	36.01	6.5564
			3200.00	37.18	6.5703
			3400.00	38.94	6.5802
			3645.00	38.01	6.5799
			3650.00	49.84	6.6976
			3889.05	52.11	6.7169
			4000.00	51.69	6.7134
			4101.74	52.28	6.7183
			4200.00	51.78	6.7142
			4340.47	50.23	6.7010
			4600.00	47.63	6.6779
			4861.33	44.72	6.6505
			5150.00	42.27	6.6260
			5385.37	40.32	6.6050
			5560.00	38.48	6.5852
			5895.92	35.55	6.5508
			6050.00	34.09	6.5326
			6562.82	29.95	6.4764
			7000.00	26.66	6.4259
			7460.00	23.69	6.3746

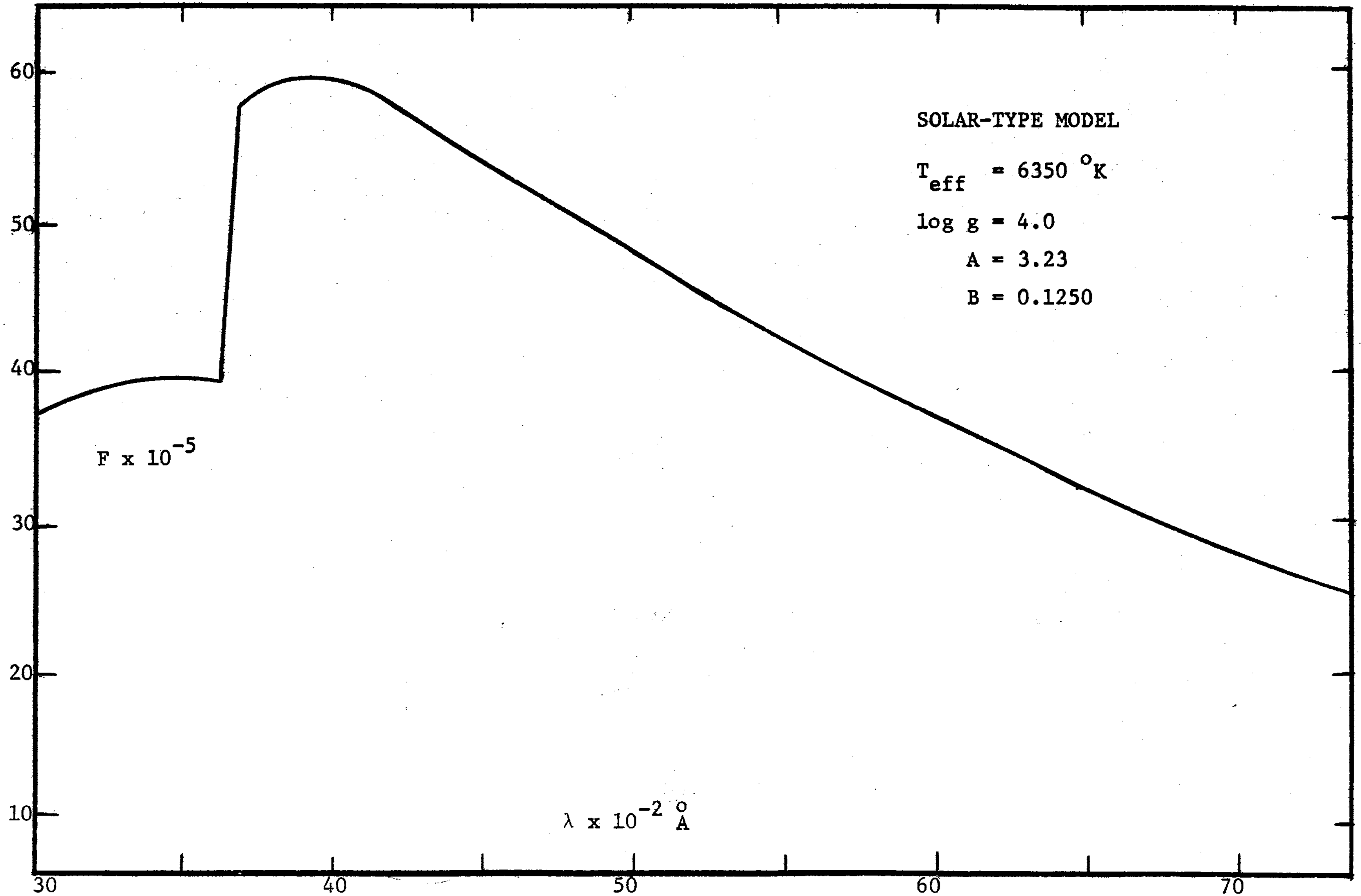

Figure 1. Theoretical Flux Distribution

values of the flux, read from the plotted figure, and then tabulated. A graph of $F(\lambda)\ S(\lambda)$ versus λ is shown in Figure 2 where the summations of $F(\lambda)\ S(\lambda)$ are the areas under the curves in this figure. Instead of a numerical integration, a summation process employing a desk calculator was used to evaluate these areas. This procedure enables one to calculate the u-b and b-v values from Equations (3-5) and (3-6) where the integrals are replaced by the summations or the areas under the curves. Using the values of u-b and b-v thus obtained, the U-B and B-V colors may be calculated using Equations (3-3) and (3-4) or (3-7) and (3-8).

An objection may be raised concerning the calculations using the Matthews and Sandage method. The true $F(\lambda)$ may not be known because of the effects of line blanketing with the result that the predicted u-b colors may be in error. This objection is valid for some stars, but it is not significant for hot stars with extremely weak Fraunhofer lines. The blanketing effect is almost nil for these stars, but the effect in stars like the sun should be taken into account before using the $F(\lambda)$ function in the above equations.

The theoretical colors, neglecting line blanketing, were calculated for effective temperatures of 6200, 6350, 6500, and 6650 ^{o}K and log g = 3.8, 4.0, 4.2, and 4.4. The results of the calculations are shown in Table VI. It is evident that the computed values of the U-B and B-V colors are not in agreement with the observed colors for Theta Ursae Majoris: U-B = 0.06 and B-V = 0.46. These observed colors are from the Arizona-Tonantzintla Catalogue (Iriarte, et al, 1965). In order to determine if a model better fitting the observations could be obtained, the theoretical colors were calculated with the effects of line blanketing taken into consideration.

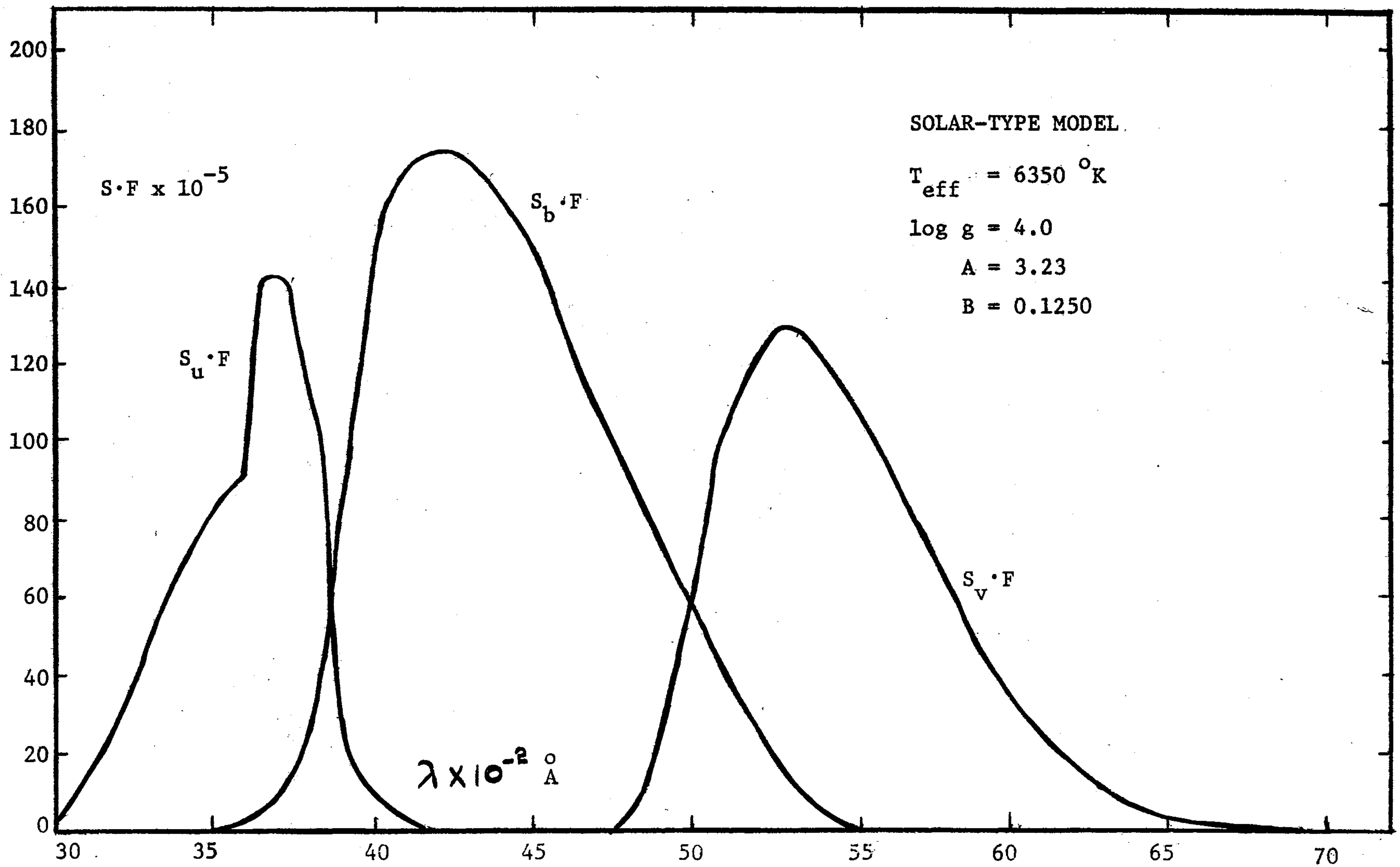

Figure 2. Theoretical Three-Color Flux Transmissions

TABLE VI

THEORETICAL COLORS WITHOUT LINE BLANKETING

Effective Temperature (^{o}K)	log g	U-B Matthews Sandage	U-B Matsushima Hall	B-V Matthews Sandage	B-V Matsushima Hall
6650	3.8	-0.305	-0.351	0.265	0.268
	4.0	-0.343	-0.377	0.266	0.269
	4.2	-0.367	-0.399	0.273	0.276
	4.4	-0.371	-0.404	0.266	0.270
6500	3.8	-0.329	-0.364	0.278	0.281
	4.0	-0.346	-0.380	0.287	0.289
	4.2	-0.379	-0.412	0.295	0.297
	4.4	-0.371	-0.404	0.289	0.292
6350	3.8	-0.337	-0.372	0.307	0.308
	4.0	-0.359	-0.365	0.304	0.305
	4.2	-0.362	-0.368	0.323	0.324
	4.4	-0.349	-0.383	0.309	0.310
6200	3.8	-0.323	-0.358	0.331	0.332
	4.0	-0.321	-0.356	0.336	0.337
	4.2	-0.353	-0.387	0.324	0.325
	4.4	-0.375	-0.401	0.334	0.334

Theoretical Colors With Line Blanketing

The first calculation of the UBV colors, with the line blanketing considered, was done using the blanketing coefficients of the star Procyon in the region between 3000 and 4200 angstroms and the blanketing coefficients of the star Gamma Serpentis in the region between 4200 and 7200 angstroms. The stars Procyon and Gamma Serpentis were selected because they are similar to the star θ Ursae Majoris which is an F6 IV star. Procyon is classified as an F5 IV-V star and Gamma Serpentis as an F6 IV-V star. Tables VII and VIII list the blanketing coefficients for the stars Gamma Serpentis (Kegel, 1962) and Procyon (Talbert and Edmonds, 1966).

TABLE VII

BLANKETING COEFFICIENTS FOR γ SERPENTIS

λ*	γ
4200	.850
4300	.840
4400	.895
4500	.910
4600	.935
4700	.945
4800	.915
4900	.950
5000	.940
5100	.925
5200	.935
5300	.950
5400	.960
5500	.965
5600	.970
5700	.980
5800	.985
5900	.990
6000	.985
6100	.975

TABLE VII (Continued)

λ*	γ
6200	.980
6300	.977
6400	.972
6500	.940
6600	.995
6700	.990
6800	.997
6900	.997
7000	.992
7100	.992
7200	.992
7300	.992
7400	.992
7500	.990

*The lower limit of the 100-Å interval is tabulated as λ.

TABLE VIII

BLANKETING COEFFICIENTS FOR PROCYON

λ*	γ
3025	.643
3050	.673
3075	.710
3100	.721
3125	.711
3150	.723
3175	.689
3200	.733
3225	.674
3250	.792
3275	.799
3300	.799
3325	.827
3350	.775
3375	.805
3400	.808
3425	.797
3450	.776
3475	.738
3500	.775

TABLE VIII (Continued)

λ^*	γ
3525	.796
3550	.761
3575	.722
3600	.718
3625	.737
3650	.805
3675	.725
3700	.675
3725	.620
3750	.638
3775	.676
3800	.748
3825	.578
3850	.785
3875	.651
3900	.780
3925	.552
3950	.615
3975	.819
4000	.762
4025	.826
4050	.841
4075	.832

*The lower limit of the 25-Å interval is tabulated as λ.

Table IX gives the calculated values of the U-B and B-V colors using the methods of Matthew and Sandage and of Matsushima and Hall. The values of the colors when line blanketing is considered are closer to observed values than in the blanketing-free case, but a discrepancy still exists between the theoretical and observed colors. An attempt will be made to reduce these differences using recently measured (Myrick, 1970) line blanketing effects for Theta Ursae Majoris.

TABLE IX

THEORETICAL COLORS WITH BLANKETING FROM GAMMA SERPENTIS AND PROCYON

Effective Temperature (°K)	log g	U-B	U-B	B-V	B-V
		Matthews Sandage	Matsushima Hall	Matthews Sandage	Matsushima Hall
6650	3.8	-0.147	-0.158	0.388	0.387
	4.0	-0.171	-0.182	0.379	0.378
	4.2	-0.188	-0.199	0.384	0.383
	4.4	-0.193	-0.203	0.380	0.379
6500	3.8	-0.154	-0.165	0.326	0.327
	4.0	-0.169	-0.180	0.399	0.397
	4.2	-0.201	-0.211	0.406	0.404
	4.4	-0.207	-0.216	0.401	0.399
6350	3.8	-0.161	-0.172	0.419	0.416
	4.0	-0.135	-0.189	0.421	0.418
	4.2	-0.193	-0.203	0.423	0.420
	4.4	-0.176	-0.186	0.421	0.418
6200	3.8	-0.145	-0.157	0.440	0.437
	4.0	-0.144	-0.156	0.436	0.432
	4.2	-0.175	-0.185	0.433	0.430
	4.4	-0.199	-0.210	0.443	0.439

The blanketing coefficient is defined according to the equation

$$\Upsilon = \int_{\lambda-\frac{\Delta\lambda}{2}}^{\lambda+\frac{\Delta\lambda}{2}} F_\lambda \, d_\lambda \Big/ F_c \, d\lambda, \tag{3-9}$$

where F_λ is the observed flux at some wavelength λ,

F_c is the corresponding continuum flux,

$\Delta\lambda$ is an arbitrary interval.

The blanketing coefficient is a measure of the fraction of the continuum flux which is emitted in the $\Delta\lambda$ band pass. The blanketing coefficient is determined by integrating Equation (3-9) or it can be determined from observational measurements.

The theoretical UBV colors, considering line blanketing, where computed again using the appropriate blanketing coefficients of θ Ursae Majoris over twenty-five angstrom intervals. The method of calculation of the UBV colors considering line blanketing is accomplished by multiplying $F(\lambda)$ $S(\lambda)$ for each twenty-five angstrom interval by the appropriate blanketing coefficient for the wavelength interval and summing the products over the entire wavelength for the desired color computed. Using this method to calculate the UBV colors, Equations (3-5) and (3-6) will become

$$u-b = 2.5 \log \frac{\int_0^\infty \Upsilon S_b(\lambda) \; F(\lambda) d\lambda}{\int_0^\infty \Upsilon S_v(\lambda) \; F(\lambda) d\lambda}, \tag{3-10}$$

$$b-v = 2.5 \log \frac{\int_0^\infty \Upsilon S_u(\lambda) \; F(\lambda) d\lambda}{\int_0^\infty \Upsilon S_b(\lambda) \; F(\lambda) d\lambda}. \tag{3-11}$$

The blanketing coefficients determined by Myrick (1970) for θ Ursae Majoris included the wavelengths from 3920 to 6610 angstroms. In order to employ appropriate blanketing coefficients between 3000 to 3920 angstroms and 6610 and 7200 angstroms, two similar stars with known blanketing coefficients were used. In the region of 3000 to 3920 angstroms an extrapolation was made using the blanketing coefficients of the star Procyon (Talbert and Edmonds, 1966). Extrapolation gave the same values for the blanketing coefficients for the two stars. In the region between 6600 and 7200 angstroms, an extrapolation was made using the blanketing coefficients of the star Gamma Serpentis (Kegel, 1962). The extrapolation found was

$$\gamma(\theta \text{ Ursae Majoris}) = 0.986\ \gamma(\text{Gamma Serpentis}). \qquad (3\text{-}11)$$

Figure 3 illustrates the difference between the theoretical flux distribution of a solar-type model star with and without line blanketing. Tables VII and VIII give the blanketing coefficients used in the extrapolations while Table X lists the blanketing coefficients used for Theta Ursae Majoris.

The intensitometer tracings used to determine the blanketing coefficients for θ Ursae Majoris include those used for the study of the hydrogen lines described in Chapter IV.

The computed values of the UBV colors for θ Ursae Majoris, using the absorption coefficients for θ Ursae Majoris, gave values that are in good agreement with the observed values of the B-V colors using three-, five-, or eight-color photometry systems. The value of B-V, for the model atmosphere with effective temperature of 6200 $^{\circ}$K and having log g = 3.8 or 4.0, is 0.46, which is the observed value given by the Lunar and Planetary Laboratory of the University of Arizona. Table XI lists the values of the U-B and B-V colors calculated by the Matthews-Sandage and

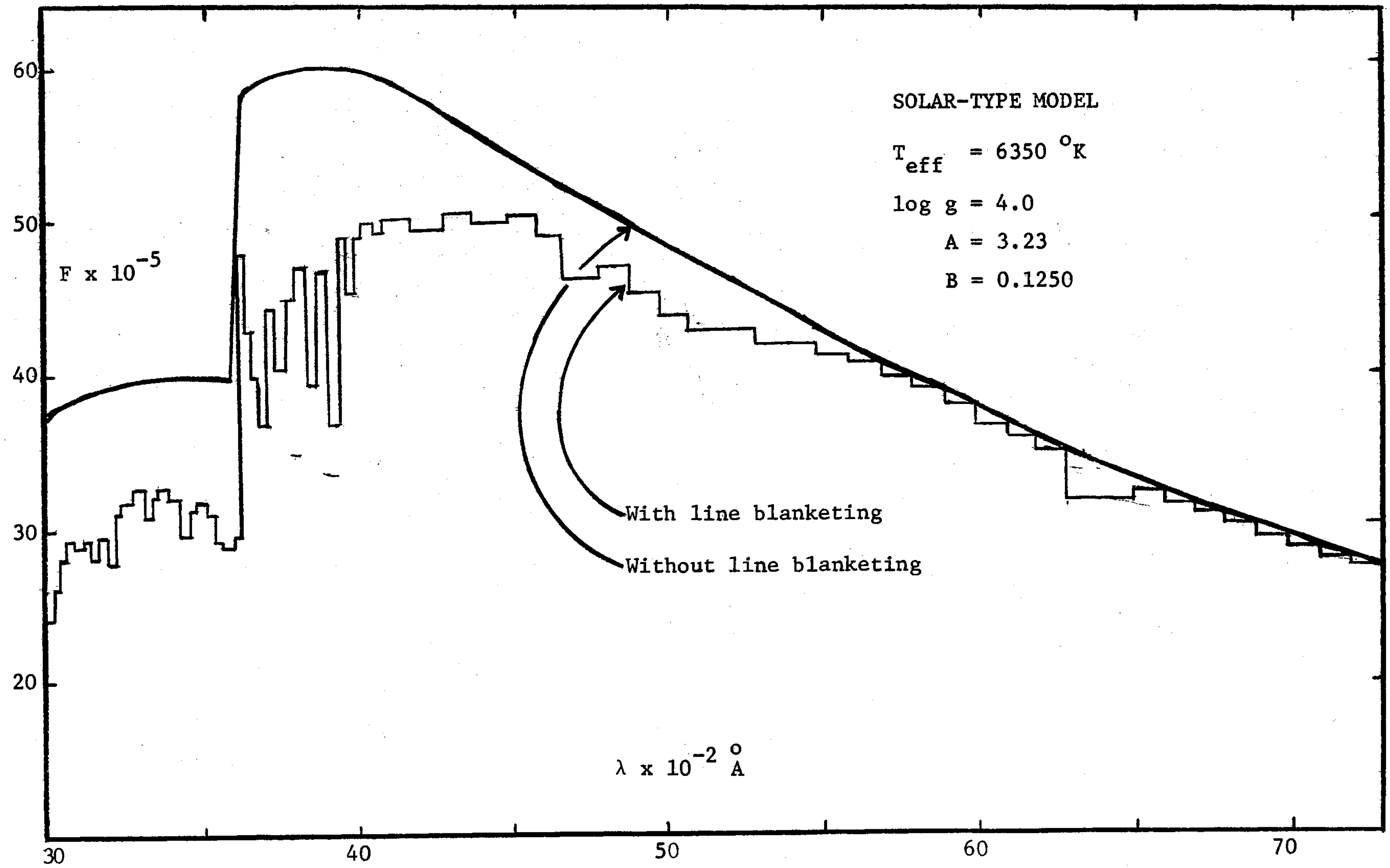

Figure 3. Theoretical Flux Distribution With Line Blanketing

TABLE X

BLANKETING COEFFICIENTS FOR θ URSAE MAJORIS (25-Å INTERVALS)

λ*	γ	λ*	γ
3025	0.643	4150	0.842
3050	0.673	4175	0.784
3075	0.710	4200	0.852
3100	0.721	4225	0.775
3125	0.711	4250	0.874
3150	0.723	4275	0.855
3175	0.689	4300	0.757
3200	0.733	4325	0.822
3225	0.674	4350	0.778
3250	0.792	4375	0.894
3275	0.799	4400	0.847
3300	0.799	4425	0.886
3325	0.827	4450	0.843
3350	0.775	4475	0.898
3375	0.805	4500	0.896
3400	0.808	4525	0.835
3425	0.797	4550	0.845
3450	0.776	4575	0.889
3475	0.738	4600	0.904
3500	0.775	4625	0.941
3525	0.796	4650	0.910
3550	0.761	4675	0.920
3575	0.722	4700	0.904
3600	0.718	4725	0.933
3625	0.737	4750	0.926
3650	0.805	4775	0.925
3675	0.725	4800	0.929
3700	0.675	4825	0.895
3725	0.620	4850	0.795
3750	0.638	4875	0.802
3775	0.676	4900	0.902
3800	0.748	4925	0.856
3825	0.578	4950	0.922
3850	0.785	4975	0.922
3875	0.651	5000	0.894
3900	0.780	5025	0.889
3925	0.572	5050	0.914
3950	0.638	5075	0.909
3975	0.489	5100	0.929
4000	0.776	5125	0.906
4025	0.829	5150	0.916
4050	0.803	5175	0.090
4075	0.774	5200	0.903
4100	0.684	5225	0.915
4125	0.826	5275	0.903
5300	0.942	6250	0.939

TABLE X (Concluded)

λ^*	γ	λ^*	γ
5325	0.914	6275	0.932
5350	0.954	6300	0.943
5375	0.928	6325	0.974
5400	0.917	6350	0.968
5425	0.928	6375	0.969
5450	0.950	6400	0.964
5475	0.924	6425	0.972
5500	0.908	6450	0.959
5525	0.931	6475	0.960
5550	0.952	6500	0.953
5575	0.950	6525	0.979
5600	0.926	6550	0.908
5625	0.951	6575	0.945
5650	0.943	6600	0.973
5675	0.961	6625	0.982
5700	0.942	6650	0.982
5725	0.960	6675	0.982
5750	0.950	6700	0.977
5775	0.946	6725	0.977
5800	0.967	6750	0.977
5825	0.988	6775	0.977
5850	0.968	6800	0.984
5875	0.988	6825	0.098
5900	0.950	6850	0.984
5925	0.703	6875	0.984
5950	0.964	6900	0.984
5975	0.975	6925	0.984
6000	0.976	6950	0.984
6025	0.960	6975	0.984
6050	0.972	7000	0.979
6075	0.971	7025	0.979
6100	0.972	7050	0.979
6125	0.948	7075	0.979
6150	0.961	7075	0.979
6175	0.954	7100	0.979
6200	0.970	7125	0.979
6225	0.964	7150	0.979
		7175	0.979
		7200	0.979

*The lower limit of the 25-Å interval is tabulated as λ.

TABLE XI

THEORETICAL COLORS WITH BLANKETING FROM θ URSAE MAJORIS

Effective Temperature (°K)	Log g	U-B	U-B	B-V	B-V
		Matthews Sandage	Matsushima Hall	Matthews Sandage	Matsushima Hall
6650	3.8	-0.201	-0.211	0.41	0.41
	4.0	-0.230	-0.259	0.42	0.41
	4.2	-0.191	-0.221	0.36	0.36
	4.4	-0.231	-0.260	0.39	0.39
6500	3.8	-0.194	-0.204	0.40	0.40
	4.0	-0.144	-0.202	0.42	0.42
	4.2	-0.224	-0.23	0.43	0.42
	4.4	-0.225	-0.244	0.40	0.40
6350	3.8	-0.181	-0.193	0.41	0.41
	4.0	-0.200	-0.210	0.42	0.41
	4.2	-0.216	-0.226	0.42	0.42
	4.4	-0.195	-0.205	0.45	0.44
6200	3.8	-0.169	-0.180	0.46	0.46
	4.0	-0.167	-0.178	0.46	0.46
	4.2	-0.201	-0.211	0.44	0.44
	4.4	-0.223	-0.233	0.44	0.43

Matsushima-Hall methods. The observed values of U-B and B-V are 0.06 and 0.46 respectively. Results will be discussed in detail in the Chapter V.

CHAPTER IV

HYDROGEN LINE PROFILES

Stellar Absorption Lines

The physical processes of line formation assume two extreme points of view. One method assumes that a unique temperature completely determines the emission and absorption processes in a given volume element and Kirchhoff's law holds. This condition is called local thermodynamic equilibrium. It is referred to as absorption and the radiation from the center of a strong line will correspond to the temperature of the uppermost stratum. The second method assumes the atoms are not in temperature equilibrium with the radiation field, but simply scatter quanta reaching them from greater depths. A particular light quantum may be absorbed and re-emitted many times on its way through the atmosphere, and since it may be thrown either backward, forward, or sideways, its chance of reaching the surface is small. A line formed according to this mechanism of scattering (also labeled monochromatic radiative equilibrium) will have a black center unless it is quite weak.

There is a tendency for resonance lines to favor the scattering mechanism and high level subordinate lines to lean toward the local thermodynamic mechanism. In the hydrogen spectrum the Lyman alpha line tends to follow the scattering mechanism, whereas the Balmer lines, and more particularly the Paschen and Brackett lines, will follow the local thermodynamic equilibrium scheme.

Formulation of the Absorption Line Program

This investigation assumes the absorption lines are formed in local thermodynamic equilibrium and the source function is the Planck function. This assumption is more valid for lines formed by absorption, than for those formed by scattering.

The formation of the equation specifying the line depth in flux is given by Gussman (1963). The line depth is given as

$$R(\Delta\lambda) = \frac{F_\lambda(0) - F_{\Delta\lambda}(0)}{F_\lambda(0)} , \qquad (4\text{-}1)$$

where $F_\lambda(0)$ = the emergent continuum flux,

$F_{\Delta\lambda}(0)$ = the emergent flux in the line at the point $\Delta\lambda$ from the line center,

and the quantity $F_\lambda(0)$ is obtained from the model atmosphere computations, It is practical to use a wavelength region of 100 or 200 Å in the computation of the line depth because the continuum intensity is not a strong variable with wavelength throughout the visible region, except near absorption discontinuities. In order to calculate the line depth the quantity $F_{\Delta\lambda}(0)$ must be determined.

A gradient method which was modified by Evans (1966) was used in calculating the line depth. This method gives the line depth as

$$R(\Delta\lambda) = \int_{-\infty}^{\infty} \frac{dB_\lambda}{dx} \left[E_3(\tau_\lambda) - E_3(\tau_\lambda + \tau_\ell)\right] \frac{2}{F_\lambda(0)} \, dx, \qquad (4\text{-}2)$$

where $\tau_\ell(x,\Delta\lambda)$ = the optical depth in the line and it is given by

$$\tau_\ell(x,\Delta\lambda) = \int_{-\infty}^{x} \frac{\kappa\ell}{\kappa_o} \left[\frac{\tau_o}{\text{Mod}}\right] dx , \qquad (4\text{-}3)$$

$\kappa_\ell(x,\Delta\lambda)$ = the line absorption coefficient per hydrogen particle,

$$B_\lambda = \frac{2hc^2}{\lambda^5}\left[\frac{1}{e^{hc/\lambda\kappa t}-1}\right] , \quad (4\text{-}4)$$

$$\frac{dB_\lambda}{dx} = \left(\frac{B_\lambda(x+\Delta x) - B_\lambda(x-\Delta x)}{2\Delta x}\right) , \quad (4\text{-}5)$$

and $\kappa_o(x)$ and $\tau_o(x)$ are obtained from the model atmosphere calculations. If $\tau_\ell << \tau_\lambda$, a Taylor expansion is used for E_3 resulting in

$$E_3(\tau_\lambda) - E_3(\tau_\lambda + \tau_\ell) = \tau_\ell E_2(\tau_\lambda); \quad (4\text{-}6)$$

$\tau_\lambda \simeq \tau_\ell$, the straight difference is computed;

$\tau_\lambda << \tau_\ell$, the approximation is made

$$E_3(\tau_\lambda) - E_3(\tau_\lambda + \tau_\ell) = E_3(\tau_\lambda) . \quad (4\text{-}7)$$

The line absorption coefficient is computed as a function of $\Delta\lambda$ and x so that the integrand of the optical depth in the line [Equation (4-3)] can be formed.

The line depth integration is performed by a summation over the desired integration range. The integrand decreases rapidly in the outer and deeper layers making this method quite accurate. The mean depth of formation is found by multiplying the line depth integrand by x, summing over the integration range, and dividing by the line depth.

The problem of calculation of the line depth reduces to the specification of the absorption coefficient in the line and its variation with $\Delta\lambda$.

Hydrogen Line Absorption Coefficient

The core of the Balmer lines are formed above x = -3.0 where deviations from local thermodynamic equilibrium are important. Since this study is concerned with the wings of the Balmer lines, Doppler broadening and radiation damping are neglected because they are negligible when compared to linear Stark broadening.

A complete formulation, computer program, derivations, and theory of the hydrogen line absorption coefficient is not given in this study due to the length of a complete discussion of each of the programs. A detailed description of the hydrogen line absorption coefficient is given by Evans (1966). This study will summarize some of the most important formulations, equations, assumptions, the computer program, and select a formulation that will be used to compute the Hα, Hβ, Hγ, and Hδ lines.

The line absorption coefficient per hydrogen particle may be written as (Aller 1963a).

$$\kappa_{\ell}(x,\Delta\lambda) = [1 - 10^{x_{\lambda}\theta}] \frac{N}{N_H} \frac{\sqrt{\pi} e^2}{mc^2} \frac{\lambda^2}{\Delta\lambda_D} f\phi_{\Delta\lambda}, \qquad (4\text{-}8)$$

where $(1 - 10^{-x_{\lambda}\theta})$ = the correction for simulated emission,

N = the number of absorbing particles in the lower level of the transition of interest per unit volume,

N_H = the number of hydrogen particles per unit volume,

$\Delta\lambda_D$ = the Doppler width $= \frac{\lambda}{c}\sqrt{E_{th}^2 + E_t^2}$,

E_{th} = the most probable thermal velocity,

$= 2RT/\mu_i = 83.83/\mu_i\theta$,

E_i = the most probable microturbulent velocity,

f = the oscillator strength,

$\phi_{\Delta\lambda}$ = the broadening function.

The number of absorbing particles per unit volume, N, is obtained from a system of Saha and Boltzman equations and may be written as

$$N = \left(\frac{n_{p,s}}{n_q}\right)\left(\frac{n_p}{\Sigma n_q}\right) Ni \qquad (4\text{-}9)$$

where $n_{p,s}$ = the number density of particles in the p-th ionization stage and the s-th excitation stage,

Σn_q = the summation over all ionization stages,

$= N_i$.

Equation (4-8) is simplified by Evans (1966) by letting r be the most abundant ionization state for the temperature and pressure of interest, r-1 the ionization stage below r, r + 1 the ionization stage above r, U_r the partition function of the r-th stage of ionization, and $q_{p,s}$ the statistical weight of the lower level. Equation (4-8) may be written as

$$\kappa_\ell = \frac{\varepsilon i \sqrt{\pi} e^2}{mc^2} \frac{\lambda^2}{\Delta\lambda_D} \frac{g_{p,s}}{U} [10^{\Delta\chi\theta} + h(9.0301 - 2.5 \log \theta - \log P_e] \qquad (4\text{-}10)$$

$$[1 - 10^{-\chi_\lambda \theta}] [f\phi],$$

h = -1 if p = $r-1$,

h = 0 if $p = r$,

h = +1 if $p = r + 1$,

$\chi_{r,s}$ = the excitation potential in eV,

$$U = U_r\left[\frac{n_{r-1}}{n_r} + 1 + \frac{n_{r+1}}{n_r}\right].$$

$$\log\left(\frac{n_{p,s}U_n}{n_r}\right) = \log g_{p,s} + \Delta\chi\theta + h\,[9.0801 - 2.5\log\theta - \log P_e]. \quad (4\text{-}11)$$

Griem Formulation

The Griem, Kolb, and Shen (1959) formulation is used here for the electron broadening. This formulation utilized the impact theory of Baranger (1958) for electron broadening along with a modification of the Holtsmark ion field distribution including Debye shielding, ion-ion correlations, and non-adiabatic transitions. The improvement in the ion field distribution effects only the line core and is unimportant for the wings. This study used the Griem, Kolb, and Shen formulation of the absorption coefficient of hydrogen to compute the Balmer lines Hα, Hβ, Hγ, and Hδ. Griem (1962) made an additional modification for quasi-static treatment of the electron fields in the far wings. This latter modification is the one most used by astrophysicists.

Computer Program for the Balmer Lines

A detailed description of the hydrogen line program is given by Evans (1966). Some modifications were made in order for the program to compute more lines and to compute more points in order to improve the accuracy of the hydrogen lines. The model atmosphere program described in Chapter II generated output needed in the hydrogen line programs. At twenty-seven different depths in the atmosphere, the output on punched data cards included the mean molecular weight and logarithms of the electron pressure, the gas pressure, the density, and the ratio of the absorption coefficient, κ_o, to the electron pressure.

The wings of the Balmer lines, Hα, Hβ, Hγ, and Hδ were computed for each of our 16 atmospheric models. These data are tabulated in Table XII where the line depth in terms of the continuum as unity is listed as a function of $\Delta\lambda$, distance from the line center, beginning with one angstrom and extending to nineteen angstroms in intervals of two angstroms.

Spectrograms and Tracings

The spectrograms used in this study were taken at the Cassegrain focus of the seventy-two inch telescope of the Dominion Astrophysical Observatory by Dr. K. O. Wright.

The dispersion of the different spectrographs ranged from 7.5 A/mm, for the second order spectra in the range $\lambda\lambda$4800-6750 for the Littrow spectrograph with a Wood grating (15,000 lines/inch), 4.5 A/mm for the third order spectra in the range $\lambda\lambda$3750-4500, 3.2 A/mm in the second order for the Baush and Lomb grating No. 496(30,000 lines/inch), and for the three-prism spectrograph the variation was from 5 A/mm to 15 A/mm over the entire wavelength range under consideration.

The intensitometer and microphotometer tracings were done by Dr. L. W. Schroeder at Victoria, Canada. The magnification of the tracings is 200. Data concerning the wavelength range, Victoria plate number, microphotometer and intensitometer tracings numbers and spectrographs, used in this investigation can be obtained from the Physics Department of Oklahoma State University at Stillwater, Oklahoma.

Comparison With Observations

Measurements were made of all the Balmer line profiles represented by the intensitometer tracings described in the previous section. The

TABLE XII

COMPUTED VALUES FOR HYDROGEN LINE PROFILES

H_δ	λ4101.74			F4 V			T_{eff} = 6650 ^{o}K				log g = 3.8
$\Delta\lambda$	1.0	3.0	5.0	7.0	9.0	11.0	13.0	15.0	17.0	19.0	21.0	23.0
Line Depth	0.48950	0.28827	0.19784	0.14368	0.10880	0.08442	0.06652	0.05313	0.04291	0.03498	0.02876	0.02382

H_γ	λ4340.47			F4 V			T_{eff} = 6650 ^{o}K				log g = 3.8
$\Delta\lambda$	1.0	3.0	5.0	7.0	9.0	11.0	13.0	15.0	17.0	19.0	21.0	23.0
Line Depth	0.46800	0.27373	0.18764	0.13707	0.10416	0.08153	0.06498	0.05251	0.04295	0.03550	0.02961	0.02489

H_β	λ4861.33			F4 V			T_{eff} = 6650 ^{o}K				log g = 3.8
$\Delta\lambda$	1.0	3.0	5.0	7.0	9.0	11.0	13.0	15.0	17.0	19.0	21.0	23.0
Line Depth	0.42776	0.24557	0.16678	0.12218	0.09294	0.07274	0.05831	0.04757	0.03929	0.03280	0.02764	0.02349

H_α	λ6562.82			F4 V			T_{eff} = 6650 ^{o}K				log g = 3.8
$\Delta\lambda$	1.0	3.0	5.0	7.0	9.0	11.0	13.0	15.0	17.0	19.0	21.0	23.0
Line Depth	0.34463	0.18807	0.12301	0.08696	0.06464	0.04965	0.03903	0.03129	0.02552	0.02111	0.01768	0.01496

TABLE XII (Continued)

H_δ		λ4101.74			F4 V			T_{eff} = 6650 °K				log g = 4.0
$\Delta\lambda$	1.0	3.0	5.0	7.0	9.0	11.0	13.0	15.0	17.0	19.0	21.0	23.0
Line Depth	0.48895	0.28760	0.19732	0.14332	0.10864	0.08445	0.06668	0.05336	0.04318	0.03527	0.02905	0.02413
H_γ		λ4340.47			F4 V			T_{eff} = 6650 °K				log g = 4.0
$\Delta\lambda$	1.0	3.0	5.0	7.0	9.0	11.0	13.0	15.0	17.0	19.0	21.0	23.0
Line Depth	0.46771	0.27339	0.18738	0.13696	0.10415	0.08165	0.06520	0.05278	0.04326	0.03581	0.02992	0.02520
H_β		λ4861.33			F4 V			T_{eff} = 6650 °K				log g = 4.0
$\Delta\lambda$	1.0	3.0	5.0	7.0	9.0	11.0	13.0	15.0	17.0	19.0	21.0	23.0
Line Depth	0.42876	0.24568	0.16692	0.12239	0.09320	0.07301	0.05860	0.04778	0.03962	0.03313	0.02798	0.02381
H_α		λ6562.82			F4 V			T_{eff} = 6650 °K				log g = 4.0
$\Delta\lambda$	1.0	3.0	5.0	7.0	9.0	11.0	13.0	15.0	17.0	19.0	21.0	23.0
Line Depth	0.34611	0.18949	0.12426	0.08806	0.06563	0.05054	0.03982	0.03199	0.02614	0.02167	0.01818	0.01541

TABLE XII (Continued)

H_δ		λ4104.74			F4 V			T_{eff} = 6650 ^oK				log g = 4.2
$\Delta\lambda$	1.0	3.0	5.0	7.0	9.0	11.0	13.0	15.0	17.0	19.0	21.0	23.0
Line Depth	0.48847	0.28697	0.19679	0.14292	0.10840	0.08439	0.06673	0.05348	0.04335	0.03547	0.02926	0.02433
H_γ		λ4104.74			F4 V			T_{eff} = 6650 ^oK				log g = 4.2
$\Delta\lambda$	1.0	3.0	5.0	7.0	9.0	11.0	13.0	15.0	17.0	19.0	21.0	23.0
Line Depth	0.46747	0.27309	0.18714	0.13684	0.10411	0.08173	0.06537	0.05301	0.04350	0.03608	0.03019	0.02546
H_β		λ4340.47			F4 V			T_{eff} = 6650 ^oK				log g = 4.2
$\Delta\lambda$	1.0	3.0	5.0	7.0	9.0	11.0	13.0	15.0	17.0	19.0	21.0	23.0
Line Depth	0.42795	0.24579	0.16706	0.12257	0.09343	0.07326	0.05888	0.04817	0.03993	0.03344	0.02826	0.02409
H_α		λ4861.33			F4 V			T_{eff} = 6650 ^oK				log g = 4.2
$\Delta\lambda$	1.0	3.0	5.0	7.0	9.0	11.0	13.0	15.0	17.0	19.0	21.0	23.0
Line Depth	0.34755	0.19083	0.12543	0.08907	0.06651	0.05132	0.04050	0.03260	0.02669	0.02216	0.01852	0.01581

TABLE XII (Continued)

H_δ		λ4104.74			F4 V			T_{eff} = 6650 °K				log g = 4.4
$\Delta\lambda$	1.0	3.0	5.0	7.0	9.0	11.0	13.0	15.0	17.0	19.0	21.0	23.0
Line Depth	0.48806	0.28643	0.19631	0.15254	0.10816	0.08430	0.06674	0.05356	0.04347	0.03562	0.02943	0.02450
H_γ		λ4340.47			F4 V			T_{eff} = 6650 °K				log g = 4.4
$\Delta\lambda$	1.0	3.0	5.0	7.0	9.0	11.0	13.0	15.0	17.0	19.0	21.0	23.0
Line Depth	0.46727	0.27280	0.18689	0.13667	0.10400	0.08172	0.06544	0.05313	0.04366	0.03624	0.03036	0.02563
H_β		λ4861.33			F4 V			T_{eff} = 6650 °K				log g = 4.4
$\Delta\lambda$	1.0	3.0	5.0	7.0	9.0	11.0	13.0	15.0	17.0	19.0	21.0	23.0
Line Depth	0.42807	0.24591	0.16719	0.12273	0.09361	0.07344	0.05908	0.04839	0.04016	0.03368	0.02850	0.02431
H_α		λ6562.82			F4 V			T_{eff} = 6650 °K				log g = 4.4
$\Delta\lambda$	1.0	3.0	5.0	7.0	9.0	11.0	13.0	15.0	17.0	19.0	21.0	23.0
Line Depth	0.34895	0.19214	0.12654	0.09003	0.06734	0.05204	0.04114	0.03317	0.02719	0.02262	0.01903	0.01619

TABLE XII (Continued)

H_δ		$\lambda 4104.74$		F5 V			T_{eff} = 6500 °K				log g = 3.8	
$\Delta\lambda$	1.0	3.0	5.0	7.0	9.0	11.0	13.0	15.0	17.0	19.0	21.0	23.0
Line Depth	0.46110	0.25855	0.17294	0.12220	0.09104	0.06944	0.05396	0.04258	0.03402	0.02749	0.02241	0.01844
H_γ		$\lambda 4340.47$		F5 V			T_{eff} = 6500 °K				log g = 3.8	
$\Delta\lambda$	1.0	3.0	5.0	7.0	9.0	11.0	13.0	15.0	17.0	19.0	21.0	23.0
Line Depth	0.44040	0.24527	0.16359	0.11657	0.08737	0.06741	0.05300	0.04235	0.03431	0.02811	0.02327	0.01943
H_β		$\lambda 4861.33$		F5 V			T_{eff} = 6500 °K				log g = 3.8	
$\Delta\lambda$	1.0	3.0	5.0	7.0	9.0	11.0	13.0	15.0	17.0	19.0	21.0	23.0
Line Depth	0.40186	0.22035	0.14554	0.10428	0.07786	0.06027	0.04785	0.03863	0.03162	0.02619	0.02192	0.01851
H_α		$\lambda 6562.82$		F5 V			T_{eff} = 6500 °K				log g = 3.8	
$\Delta\lambda$	1.0	3.0	5.0	7.0	9.0	11.0	13.0	15.0	17.0	19.0	21.0	23.0
Line Depth	0.32455	0.16905	0.10771	0.07478	0.05485	0.04158	0.03236	0.02577	0.02090	0.01721	0.01435	0.01209

TABLE XII (Continued)

H_δ		λ4101.74			F5 V			T_{eff} = 6500 ^oK			log g = 4.0	
$\Delta\lambda$	1.0	3.0	5.0	7.0	9.0	11.0	13.0	15.0	17.0	19.0	21.0	23.0
Line Depth	0.46070	0.25800	0.17152	0.12189	0.09092	0.06947	0.05405	0.04272	0.03420	0.02767	0.02259	0.01861
H_γ		λ4340.47			F5 V			T_{eff} = 6500 ^oK			log g = 4.0	
$\Delta\lambda$	1.0	3.0	5.0	7.0	9.0	11.0	13.0	15.0	17.0	19.0	21.0	23.0
Line Depth	0.44021	0.24498	0.16336	0.11642	0.08733	0.06748	0.05314	0.04253	0.03450	0.02831	0.02347	0.01963
H_β		λ4861.33			F5 V			T_{eff} = 6500 ^oK			log g = 4.0	
$\Delta\lambda$	1.0	3.0	5.0	7.0	9.0	11.0	13.0	15.0	17.0	19.0	21.0	23.0
Line Depth	0.40198	0.22046	0.14565	0.01044	0.07902	0.06045	0.04806	0.03886	0.03185	0.02642	0.02214	0.01872
H_α		λ6562.82			F5 V			T_{eff} = 6500 ^oK			log g = 4.0	
$\Delta\lambda$	1.0	3.0	5.0	7.0	9.0	11.0	13.0	15.0	17.0	19.0	21.0	23.0
Line Depth	0.32597	0.17031	0.10876	0.07567	0.05562	0.04224	0.03295	0.02629	0.02136	0.01762	0.01471	0.01242

TABLE XII (Continued)

H_δ		λ4104.74			F5 V			T_{eff} = 6500 °K				log g = 4.2
Δλ	1.0	3.0	5.0	7.0	9.0	11.0	13.0	15.0	17.0	19.0	21.0	23.0
Line Depth	0.46036	0.25746	0.17106	0.12153	0.09075	0.06942	0.05410	0.03282	0.03432	0.02780	0.02273	0.01875
H_γ		λ4340.47			F5 V			T_{eff} = 6500 °K				log g = 4.2
Δλ	1.0	3.0	5.0	7.0	9.0	11.0	13.0	15.0	17.0	19.0	21.0	23.0
Line Depth	0.44005	0.24471	0.16315	0.11627	0.08727	0.06753	0.05325	0.04267	0.03466	0.02849	0.02364	0.01979
H_β		λ4861.33			F5 V			T_{eff} = 6500 °K				log g = 4.2
Δλ	1.0	3.0	5.0	7.0	9.0	11.0	13.0	15.0	17.0	19.0	21.0	23.0
Line Depth	0.40211	0.22054	0.14573	0.10454	0.07814	0.06060	0.04824	0.03907	0.03206	0.02663	0.02234	0.01892
H_α		λ6562.82			F5 V			T_{eff} = 6500 °K				log g = 4.2
Δλ	1.0	3.0	5.0	7.0	9.0	11.0	13.0	15.0	17.0	19.0	21.0	23.0
Line Depth	0.32734	0.17153	0.10976	0.07652	0.05634	0.04287	0.03349	0.02677	0.02179	0.01800	0.01506	0.01274

TABLE XII (Continued)

H_δ		$\lambda 4101.74$			F5 V			T_{eff} = 6500 °K				log g = 4.4
$\Delta\lambda$	1.0	3.0	5.0	7.0	9.0	11.0	13.0	15.0	17.0	19.0	21.0	23.0
Line Depth	0.46010	0.25704	0.17069	0.12122	0.09058	0.06936	0.05408	0.04285	0.03438	0.02790	0.02284	0.01886

H_γ		$\lambda 4340.47$			F5 V			T_{eff} = 6500 °K				log g = 4.4
$\Delta\lambda$	1.0	3.0	5.0	7.0	9.0	11.0	13.0	15.0	17.0	19.0	21.0	23.0
Line Depth	0.43994	0.24448	0.16295	0.11610	0.08718	0.06753	0.05330	0.04276	0.03477	0.02860	0.02377	0.01993

H_β		$\lambda 4861.33$			F5 V			T_{eff} = 6500 °K				log g = 4.4
$\Delta\lambda$	1.0	3.0	5.0	7.0	9.0	11.0	13.0	15.0	17.0	19.0	21.0	23.0
Line Depth	0.40225	0.22064	0.14581	0.10465	0.07825	0.06072	0.04839	0.03923	0.03223	0.02680	0.02250	0.01907

H_α		$\lambda 6562.82$			F5 V			T_{eff} = 6500 °K				log g = 4.4
$\Delta\lambda$	1.0	3.0	5.0	7.0	9.0	11.0	13.0	15.0	17.0	19.0	21.0	23.0
Line Depth	0.32871	0.17272	0.11072	0.07730	0.05700	0.04342	0.03396	0.02718	0.02215	0.01832	0.01534	0.01298

TABLE XII (Continued)

H_δ λ4101.74 F6 V T_{eff} = 6350 °K log g = 3.8

Δλ	1.0	3.0	5.0	7.0	9.0	11.0	13.0	15.0	17.0	19.0	21.0	23.0
Line Depth	0.43013	0.22928	0.14674	0.10240	0.07472	0.05597	0.04286	0.03339	0.02638	0.02109	0.01704	0.01392

H_γ λ4330.47 F6 V T_{eff} = 6350 °K log g = 3.8

Δλ	1.0	3.0	5.0	7.0	9.0	11.0	13.0	15.0	17.0	19.0	21.0	23.0
Line Depth	0.41062	0.21702	0.13976	0.00757	0.07193	0.05453	0.04227	0.03337	0.02675	0.02173	0.01784	0.01479

H_β λ4861.33 F6 V T_{eff} = 6350 °K log g = 3.8

Δλ	1.0	3.0	5.0	7.0	9.0	11.0	13.0	15.0	17.0	19.0	21.0	23.0
Line Depth	0.37405	0.10453	0.12505	0.08711	0.06409	0.04906	0.03846	0.03069	0.02488	0.02043	0.01698	0.01425

H_α λ6562.82 F6 V T_{eff} = 6350 °K log g = 3.8

Δλ	1.0	3.0	5.0	7.0	9.0	11.0	13.0	15.0	17.0	19.0	21.0	23.0
Line Depth	0.39283	0.14995	0.09266	0.06323	0.04555	0.03406	0.02628	0.02079	0.01676	0.01372	0.01139	0.00956

TABLE XII (Continued)

H_δ			$\lambda 4104.74$			F6 V		T_{eff} = 6350 °K			log g = 4.0	
$\Delta\lambda$	1.0	3.0	5.0	7.0	9.0	11.0	13.0	15.0	17.0	19.0	21.0	23.0
Line Depth	0.42987	0.22882	0.14632	0.10211	0.07459	0.05592	0.04286	0.03343	0.02646	0.02118	0.01713	0.01400

H_γ			$\lambda 4340.47$			F6 V		T_{eff} = 6350 °K			log g = 4.0	
$\Delta\lambda$	1.0	3.0	5.0	7.0	9.0	11.0	13.0	15.0	17.0	19.0	21.0	23.0
Line Depth	0.41052	0.21679	0.13959	0.09747	0.07196	0.05463	0.04241	0.03353	0.02692	0.02189	0.01799	0.01494

H_β			$\lambda 4861.33$			F6 V		T_{eff} = 6350 °K			log g = 4.0	
$\Delta\lambda$	1.0	3.0	5.0	7.0	9.0	11.0	13.0	15.0	17.0	19.0	21.0	23.0
Line Depth	0.37421	0.19462	0.12512	0.08720	0.06418	0.04919	0.03862	0.03085	0.02503	0.02058	0.01712	0.01440

H_α			$\lambda 6562.82$			F6 V		T_{eff} = 6350 °K			log g = 4.0	
$\Delta\lambda$	1.0	3.0	5.0	7.0	9.0	11.0	13.0	15.0	17.0	19.0	21.0	23.0
Line Depth	0.30419	0.15109	0.09357	0.06397	0.04616	0.03458	0.02674	0.02118	0.01710	0.01402	0.01165	0.00979

TABLE XII (Continued)

H_δ		λ4101.74			F6 V			T_{eff} = 6350 °K			log g = 4.2	
$\Delta\lambda$	1.0	3.0	5.0	7.0	9.0	11.0	13.0	15.0	17.0	19.0	21.0	23.0
Line Depth	0.42968	0.22843	0.14597	0.10118	0.07450	0.05591	0.04290	0.03351	0.02655	0.02127	0.01723	0.01410
H_γ		λ4340.47			F6 V			T_{eff} = 6350 °K			log g = 4.2	
$\Delta\lambda$	1.0	3.0	5.0	7.0	9.0	11.0	13.0	15.0	17.0	19.0	21.0	23.0
Line Depth	0.41047	0.21659	0.13941	0.09732	0.07191	0.05464	0.04244	0.03359	0.02699	0.02196	0.01806	0.01500
H_β		λ4861.33			F6 V			T_{eff} = 6350 °K			log g = 4.2	
$\Delta\lambda$	1.0	3.0	5.0	7.0	9.0	11.0	13.0	15.0	17.0	19.0	21.0	23.0
Line Depth	0.37437	0.19470	0.12520	0.08728	0.06427	0.04930	0.02875	0.03101	0.02519	0.02074	0.01727	0.01500
H_α		λ6562.82			F6 V			T_{eff} = 6350 °K			log g = 4.2	
$\Delta\lambda$	1.0	3.0	5.0	7.0	9.0	11.0	13.0	15.0	17.0	19.0	21.0	23.0
Line Depth	0.30553	0.15220	0.09443	0.06467	0.04674	0.03506	0.02715	0.02154	0.01742	0.01430	0.01190	0.01001

TABLE XII (Continued)

H_δ		$\lambda 4104.74$			F6 V		T_{eff} = 6350 ^oK				log g = 4.4	
$\Delta\lambda$	1.0	3.0	5.0	7.0	9.0	11.0	13.0	15.0	17.0	19.0	21.0	23.0
Line Depth	0.42954	0.22810	0.14567	0.10167	0.07441	0.05589	0.04293	0.03356	0.02660	0.02134	0.01730	0.01417
H_γ		$\lambda 4340.47$			F6 V		T_{eff} = 6350 ^oK				log g = 4.4	
$\Delta\lambda$	1.0	3.0	5.0	7.0	9.0	11.0	13.0	15.0	17.0	19.0	21.0	23.0
Line Depth	0.41004	0.21641	0.13925	0.09721	0.07189	0.05469	0.04252	0.03369	0.02710	0.02209	0.01819	0.01513
H_β		$\lambda 4861.33$			F6 V		T_{eff} = 6350 ^oK				log g = 4.4	
$\Delta\lambda$	1.0	3.0	5.0	7.0	9.0	11.0	13.0	15.0	17.0	19.0	21.0	23.0
Line Depth	0.37452	0.19478	0.12525	0.08734	0.06434	0.04940	0.03887	0.03114	0.02532	0.02086	0.01739	0.01465
H_α		$\lambda 6562.82$			F6 V		T_{eff} = 6350 ^oK				log g = 4.4	
$\Delta\lambda$	1.0	3.0	5.0	7.0	9.0	11.0	13.0	15.0	17.0	19.0	21.0	23.0
Line Depth	0.30684	0.16329	0.09526	0.06532	0.04727	0.03551	0.02754	0.02188	0.01772	0.01457	0.01213	0.01022

TABLE XII (Continued)

H_δ		$\lambda 4104.74$			F8 V			T_{eff} = 6200 ^{o}K			log g = 3.8	
$\Delta\lambda$	1.0	3.0	5.0	7.0	9.0	11.0	13.0	15.0	17.0	19.0	21.0	23.0
Line Depth	0.39713	0.20013	0.12329	0.08417	0.05990	0.04402	0.03319	0.02549	0.01989	0.01573	0.01261	0.01022

H_γ		$\lambda 4340.47$			F8 V			T_{eff} = 6200 ^{o}K			log g = 3.8	
$\Delta\lambda$	1.0	3.0	5.0	7.0	9.0	11.0	13.0	15.0	17.0	19.0	21.0	23.0
Line Depth	0.37842	0.18955	0.11711	0.08035	0.05795	0.04312	0.03294	0.02569	0.02037	0.01638	0.01333	0.01098

H_β		$\lambda 4861.33$			F8 V			T_{eff} = 6200 ^{o}K			log g = 3.8	
$\Delta\lambda$	1.0	3.0	5.0	7.0	9.0	11.0	13.0	15.0	17.0	19.0	21.0	23.0
Line Depth	0.34453	0.16900	0.10509	0.07134	0.05183	0.03908	0.03018	0.02379	0.01909	0.01555	0.01282	0.01068

H_α		$\lambda 6562.82$			F8 V			T_{eff} = 6200 ^{o}K			log g = 3.8	
$\Delta\lambda$	1.0	3.0	5.0	7.0	9.0	11.0	13.0	15.0	17.0	19.0	21.0	23.0
Line Depth	0.27936	0.13103	0.07947	0.05239	0.03701	0.02738	0.02096	0.01645	0.01317	0.01072	0.00885	0.00740

TABLE XII (Continued)

H_δ		λ4101.74			F8 V			T_{eff} = 6200 °K				log g = 4.0
$\Delta\lambda$	1.0	3.0	5.0	7.0	9.0	11.0	13.0	15.0	17.0	19.0	21.0	23.0
Line Depth	0.39701	0.19981	0.12297	0.08401	0.05983	0.04401	0.03321	0.02552	0.01993	0.01578	0.01267	0.01028
H_γ		λ4340.47			F8 V			T_{eff} = 6200 °K				log g = 4.0
$\Delta\lambda$	1.0	3.0	5.0	7.0	9.0	11.0	13.0	15.0	17.0	19.0	21.0	23.0
Line Depth	0.37842	0.18937	0.11694	0.08026	0.05795	0.04316	0.03299	0.02576	0.02044	0.01644	0.01340	0.01103
H_β		λ4861.33			F8 V			T_{eff} = 6200 °K				log g = 4.0
$\Delta\lambda$	1.0	3.0	5.0	7.0	9.0	11.0	13.0	15.0	17.0	19.0	21.0	23.0
Line Depth	0.34470	0.16906	0.10513	0.07139	0.05192	0.03919	0.03032	0.02393	0.01923	0.01568	0.01295	0.01081
H_α		λ6562.82			F8 V			T_{eff} = 6200 °K				log g = 4.0
$\Delta\lambda$	1.0	3.0	5.0	7.0	9.0	11.0	13.0	15.0	17.0	19.0	21.0	23.0
Line Depth	0.28065	0.13203	0.07921	0.05295	0.03746	0.02775	0.02128	0.01672	0.01340	0.01093	0.00903	0.00756

TABLE XII (Continued)

H_δ		λ4104.74		F8 V			T_{eff} = 6200 ^oK				log g = 4.2
$\Delta\lambda$	1.0	3.0	5.0	7.0	9.0	11.0	13.0	15.0	17.0	19.0	21.0	23.0
Line Depth	0.39698	0.19957	0.12274	0.08390	0.05980	0.04402	0.03326	0.02559	0.02000	0.01585	0.01274	0.01034

H_γ		λ4340.47		F8 V			T_{eff} = 6200 ^oK				log g = 4.2
$\Delta\lambda$	1.0	3.0	5.0	7.0	9.0	11.0	13.0	15.0	17.0	19.0	21.0	23.0
Line Depth	0.37849	0.18929	0.11686	0.08026	0.05801	0.04324	0.03309	0.02585	0.02053	0.01653	0.01348	0.01111

H_β		λ4861.33		F8 V			T_{eff} = 6200 ^oK				log g = 4.2
$\Delta\lambda$	1.0	3.0	5.0	7.0	9.0	11.0	13.0	15.0	17.0	19.0	21.0	23.0
Line Depth	0.34493	0.16916	0.19520	0.07144	0.05199	0.03929	0.03043	0.02404	0.01933	0.01579	0.01304	0.01090

H_α		λ6562.82		F8 V			T_{eff} = 6200 ^oK				log g = 4.2
$\Delta\lambda$	1.0	3.0	5.0	7.0	9.0	11.0	13.0	15.0	17.0	19.0	21.0	23.0
Line Depth	0.28210	0.13312	0.0800	0.05356	0.03794	0.02815	0.02162	0.01801	0.01365	0.01114	0.00921	0.00772

TABLE XII (Concluded)

H_δ λ4104.74 F8 V T_{eff} = 6200 °K log g = 4.4

Δλ	1.0	3.0	5.0	7.0	9.0	11.0	13.0	15.0	17.0	19.0	21.0	23.0
Line Depth	0.39691	0.19931	0.12248	0.08375	0.05973	0.04400	0.03325	0.02561	0.02004	0.01589	0.01278	0.01038

H_γ λ4340.47 F8 V T_{eff} = 6200 °K log g = 4.4

Δλ	1.0	3.0	5.0	7.0	9.0	11.0	13.0	15.0	17.0	19.0	21.0	23.0
Line Depth	0.37850	0.18912	0.1167	0.08014	0.05796	0.04323	0.03310	0.02589	0.02058	0.01659	0.01354	0.01117

H_β λ4861.33 F8 V T_{eff} = 6200 °K log g = 4.4

Δλ	1.0	3.0	5.0	7.0	9.0	11.0	13.0	15.0	17.0	19.0	21.0	23.0
Line Depth	0.34507	0.16921	0.10523	0.07146	0.05204	0.03935	0.03049	0.02411	0.01940	0.01585	0.01310	0.01095

H_α λ6562.82 F8 V T_{eff} = 6200 °K log g = 4.4

Δλ	1.0	3.0	5.0	7.0	9.0	11.0	13.0	15.0	17.0	19.0	21.0	23.0
Line Depth	0.28322	0.13407	0.08071	0.05410	0.03837	0.02851	0.02191	0.01726	0.01387	0.01133	0.00938	0.00787

measured line depths were then plotted to a uniform scale as a function of distance from the line center. The 64 theoretical profiles were then plotted on transparent paper to the same scale and superposed on the observed plots in an attempt to find the best agreement or fit between theory and observations. Observations best fit by the theoretical curves of a single model are listed in Table XIII. Figures 4, 5, 6, and 7 are comparisons between the calculated hydrogen line profiles--$H\alpha$, $H\beta$, $H\gamma$, and $H\delta$--and the observed profiles for a star having an effective temperature of 6500 ^{o}K, log g = 4.2, and with the solar abundance. This is the single model in best agreement with observations.

TABLE XIII

OBSERVED HYDROGEN LINE PROFILES

Hδ	λ4101.74					Victoria Plate No. 50092									Tracing No. 1797
Δλ(Å)	0.0	0.5	1.0	1.5	2.0	2.5	3.0	3.5	4.0	6.0	8.0	10.0	12.0		
Line Depth	.8571	.6408	.5019	.4503	.3257	.2859	.2541	.2302	.2112	.1667	.1239	.0877	.0395		

Hγ	λ4340.47					Victoria Plate No. 37112									Tracing No. 1914
Δλ(Å)	0.0	0.5	1.0	1.5	2.0	2.5	3.0	3.5	4.0	6.00	8.00	10.0	12.0	14.0	16.0	18.0
Line Depth	.8741	.6775	.5191	.4122	.3569	.2987	.2753	.2214	.1975	.1326	.1011	.0902	.0730	.0455	.0267	.0115

Hβ	λ4861.33					Victoria Plate No. 38133									Tracing No. 1815
Δλ(Å)	0.0	0.5	1.0	1.5	2.0	2.5	3.0	3.5	4.0	6.0	8.0	10.0	12.0	14.0	16.0	18.0
Line Depth	.9769	.6574	.4815	.3773	.3218	.2847	.2454	.2222	.1901	.1435	.1157	.0949	.0741	.0510	.0278	.0093

Hα	λ6562.82					Victoria Plate No. 36795									Tracing No. 1819
Δλ(Å)	0.0	.05	1.0	1.5	2.0	2.5	3.0	3.5	4.0	6.0	8.0	10.0	12.0		
Line Depth	.8181	.6920	.4117	.3233	.2667	.2227	.1768	.1617	.1415	.0910	.0682	.0455	.0228		

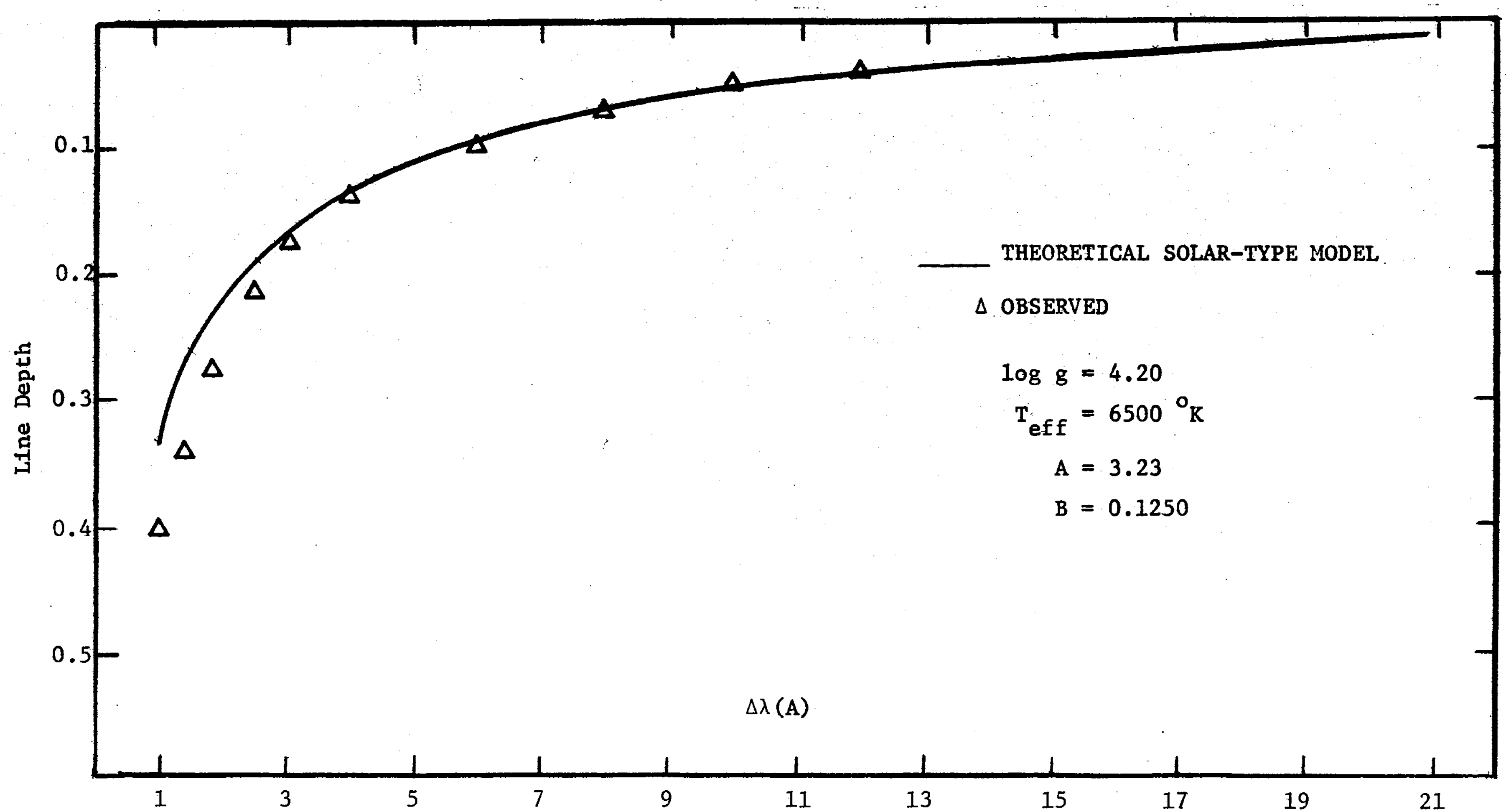

Figure 4. Observed and Theoretical Line Profiles for Hα

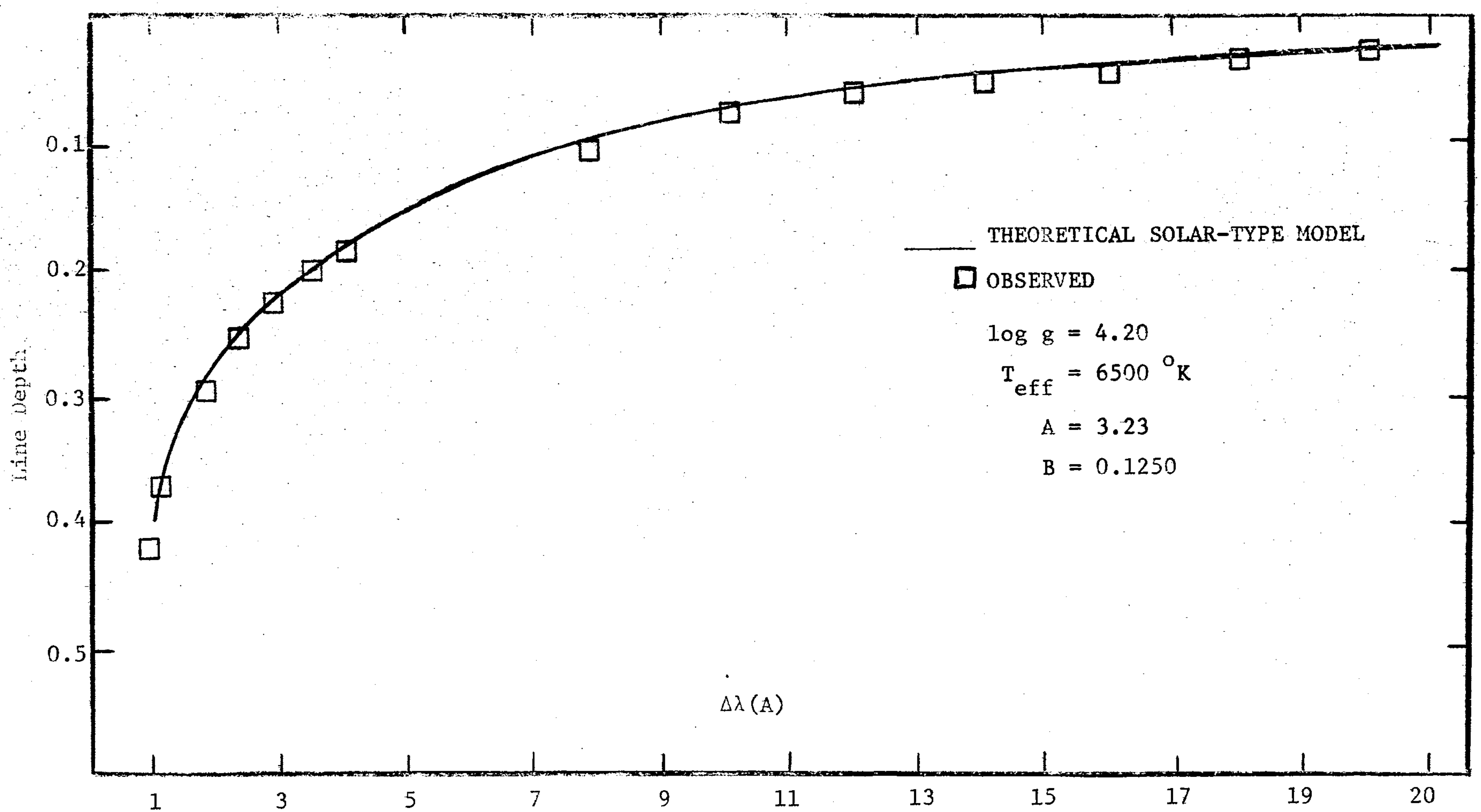

Figure 5. Observed and Theoretical Line Profiles for Hβ

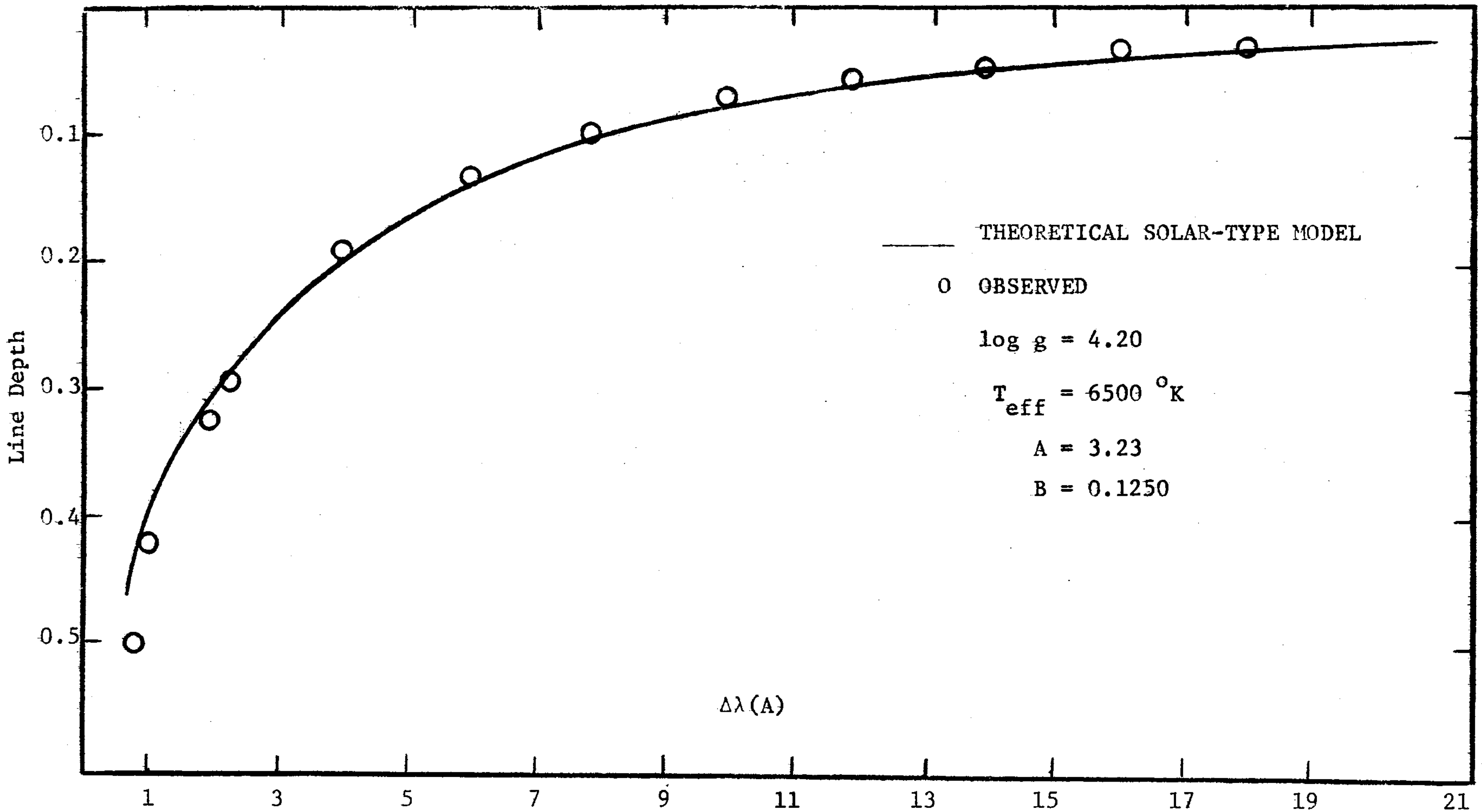

Figure 6. Observed and Theoretical Line Profiles for Hγ

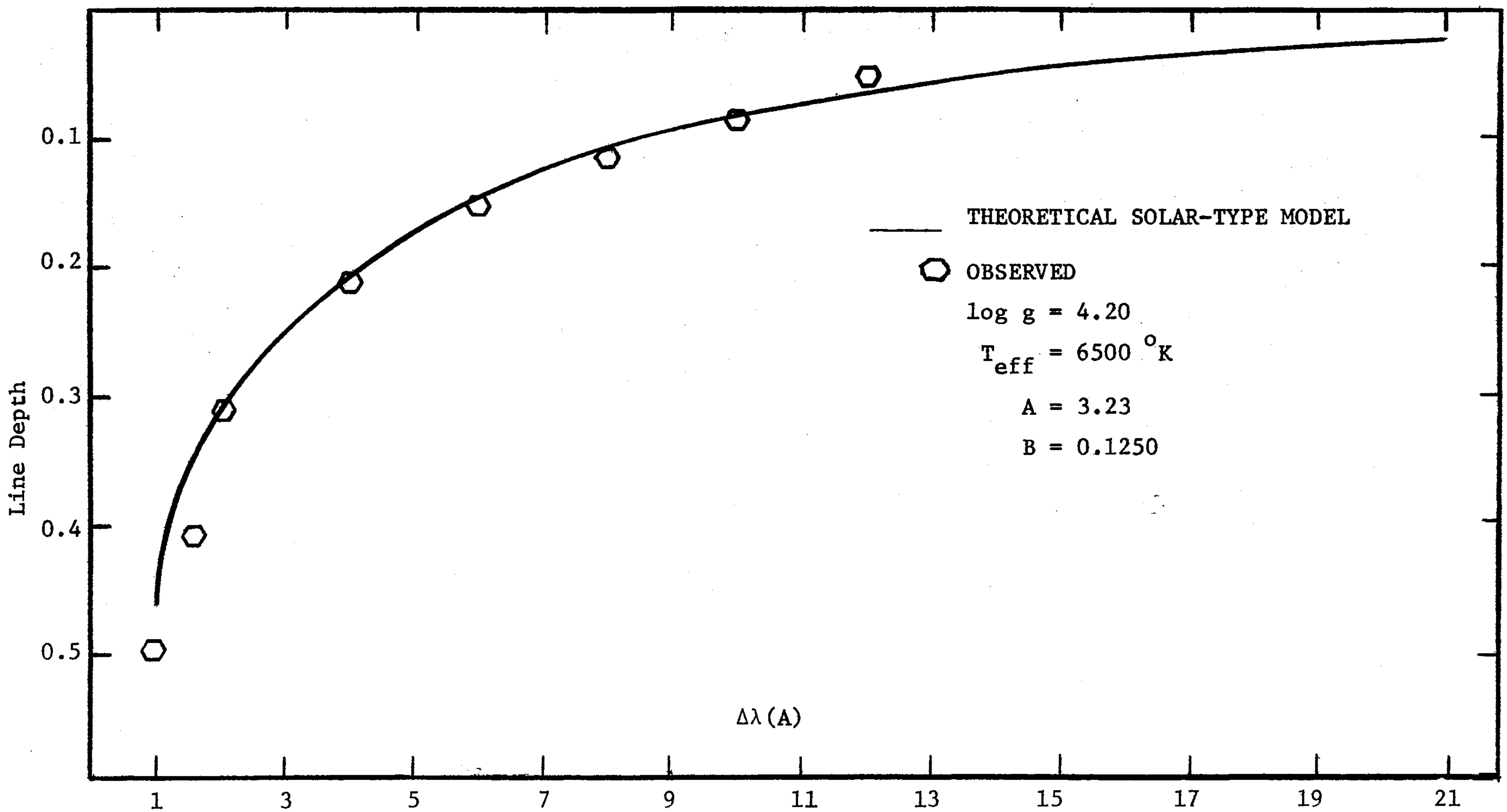

Figure 7. Observed and Theoretical Line Profiles for Hδ

CHAPTER V

SUMMARY

The Model

A detailed fine atmospheric analysis of the atmosphere of the star Theta Ursae Majoris was performed using a computer program which computes a pressure opacity-flux model for a given temperature distribution. A grid of sixteen model atmospheres, having effective temperatures between 6200 °K and 6650 °K and surface gravities between log g = 3.8 and 4.4, was calculated in order to determine if a theoretical model of the star could be developed.

Using seven basic assumptions, the theoretical UBV colors and hydrogen line profiles were calculated for the star and compared to the observed values of the UBV colors and the hydrogen line profiles to determine which model was representative of the star Theta Ursae Majoris.

Analysis of the UBV Colors

The first calculation of the UBV colors did not include the effect of line blanketing. The computed values of U-B and B-V, given in Table VI, are obviously not in agreement with the observed values of U-B = 0.06 and B-V = 0.46. Our model of the atmosphere for Theta Ursae Majoris was incorrect or line blanketing is an important factor in the computation of the UBV colors.

The second calculation of the UBV colors was performed using the blanketing coefficients from the star Procyon, given by Talbert and Edmonds (1966), in the wavelength region $\lambda = 3000$ to 4200 angstroms, and the blanketing coefficients from the star Gamma Serpentis, given by Kegel (1962), in the wavelength region $\lambda = 4200$ to 7200 angstroms. The calculated theoretical colors, using line blanketing from these similar stars, indicated a better agreement between our model and the observed values for the star, but better agreement was desired.

The third calculation of the UBV colors was performed using the blanketing coefficients for the star Theta Ursae Majoris. Myrick (1970) calculated the blanketing coefficients and factors for Theta Ursae Majoris in the wavelength region $\lambda = 3920$ to 6610 angstroms. The blanketing coefficients for the wavelength region $\lambda = 3000$ to 3920 and $\lambda =$ 6600 to 7200 angstroms were determined by extrapolation using the stars Procyon and Gamma Serpentis. Using the blanketing coefficients for the star Theta Ursae Majoris, the computed values of the UBV colors are in very good agreement with the stated values for the B-V colors. The best agreement was found to be for an F8 V model having an effective temperature of 6200 ^{o}K and surface gravity of $\log g = 3.8$ or 4.0. The computed values of the U-B colors did not show a good agreement between our model and the observed values. The poor agreement exists because the true continuum for the ultraviolet region has not been definitely established and the true values of the blanketing coefficients in this region are quite uncertain. Once the true continuum for the ultraviolet region is determined, the blanketing coefficients for this region can be determined with a high degree of accuracy. This will enable one to determine the blanketing coefficients in this wavelength region and to calculate the B-V colors with greater accuracy. The disparity between theoretical and observed U-B colors was so great that no one model could be selected as representative of the star Theta Ursae Majoris.

Analysis of the Hydrogen Line Profiles

The Balmer Hα, Hβ, Hγ, and Hδ line profiles were computed and plotted graphically for the sixteen grid models in order to compare the theoretical hydrogen line profiles with the observed profiles. This comparison was used as a criterion to determine which model would be selected as the representative model for the star Theta Ursae Majoris. The model representative of the star was an FV 5 star having an effective temperature of 6500 ^{o}K and surface gravity of log g = 4.2. Although one model might show good agreement between one observed and calculated line, the FV 5 model indicates the best agreement when all four hydrogen lines were considered.

The observed and calculated values for all four hydrogen lines are in good agreement in the wings. The Hβ and Hγ lines show good agreement as close as one angstrom from the core of the line. The agreement between observed and calculated values for the Hδ line is good when at a distance of only two angstroms from the line core. The greatest discrepancy near the center of the line core exists in the Hα line, but good agreement is obtained at a distance of three angstroms from the line core.

Conclusions

The theoretical UBV colors did not predict the same model of the star Theta Ursae Majoris as did the graphical comparison between the computed and observed values of the Balmer Hα, Hβ, Hγ, and Hδ line profiles. The model selected by the UBV colors was a star having a lower temperature, 6200 ^{o}K compared to 6500 ^{o}K, and a lower effective surface gravity, log g = 3.8 or 4.0 compared to 4.2, than the model dictated by the hydrogen line profiles. The UBV colors predict Theta Ursae Majoris to be an F8 V star while the hydrogen line profiles predict an F5 V star. Since so much disparity exists between the theoretical and observed U-B colors, the value of the U-B colors can not be used here as a good criterion to predict the model atmosphere for the star.

The blanketing coefficients for Theta Ursae Majoris in the region between 3920 and 6600 angstroms were calculated from tracings of the star itself. The blanketing coefficients in the region between 3000 to 3900 and 6600 to 7200 angstroms were calculated from similar stars and there could be an error in the calculated values of the blanketing coefficients. The use of the blanketing coefficients from similar stars could be one reason for the poor agreement between the theoretical and observed values of the U-B colors. The true continuum in the ultraviolet region has not been established with any known certainity and it is impossible to calculate the true blanketing coefficients in this region. Although our values of the U-B colors are too large by a factor of three, they show closer agreement than any other computed models for similar stars.

The hydrogen line profiles select an F5 V star as representative of Theta Ursae Majoris. This model is closer to the spectral classification of the star, F6 IV, than the model predicted by the UBV colors. It is acknowledged that there could be some error in the tracings of the hydrogen line profiles, but the probability of the error in the tracings is smaller than the error in the determination of the blanketing.

REFERENCES

Aller, L. H. 1963a, Astrophysics (2nd ed.; New York: The Ronald Press Company).

Aller, L. H. 1963b, Ap. J., 137, 690.

Athay, R. G. and Skumanich, A. 1969, Ap. J., 155, 273.

Baranger, M. 1958, Phys. Rev., 111, 481, 494; 112, 855.

Böhm, K. 1960, Stellar Atmospheres, ed. J. L. Greenstein (Chicago: University of Chicago Press), p. 88.

Elste, G. 1955, Z. f. Ap., 37, 184.

Evans, J. C. 1966, Ph.D. Thesis, University of Michigan, unpublished.

Evans, J. C., 1969, private communication.

Gingerich, O. 1964, First Harvard-Smithsonian Conference on Stellar Atmospheres (Smithsonian Special Report No. 167), p. 17.

Goldberg, L., Miller, E. A. and Aller, L. W. 1960, Ap. J. Suppl., 5, 1.

Griem, H. R. 1962, Ap. J., 136, 422.

Griem, H. R., Kolb, A., and Shen, K. Y. 1959, Phys. Rev., 116, 4.

Iriarte, B., Johnson, H. L., Mitchell, R. J., Wisniewski, W. W. 1965, Sky and Telescope, XXX, No. 1, 24.

Johnson, H. L. 1954, Ap. J., 120, 196.

Johnson, H. L. and Morgan, W. W. 1951, Ap. J., 114, 522.

Johnson, H. L. and Morgan, W. W. 1953, Ap. J., 117, 313.

Kennan, P. C. and Morgan, W. W. 1951, Astrophysics ed. J. A. Hynek (New York: McGraw-Hill Book Co.), Chp. 1.

Kegel, W. H. 1962, Zs. f. Ap., 55, 243.

Kourganoff, V. 1952, Basic Methods in Transfer Problems (Oxford: Oxford University Press).

Matsushima, S. and Hall, D. 1969, Ap. J., 156, 779.

Matthews, R. and Sandage, A. 1963, Ap. J., 138, 49.

Melbourne, W. G. 1960, Ap. J., 132, 101.

Mihalas, D. 1966, Ap. J., Suppl., 13, 1.

Myrick, E. G. 1970, Masters Thesis, Oklahoma State University, unpublished.

Talbert, F. D. and Edmonds, F. N. 1966, Ap. J., 146, 177.

Weidermann, V. 1955, Z. f. Ap., 36, 101.

VITA

John Goodson Bulman

Candidate for the Degree of Doctor of Education

Thesis: A FINE ATMOSPHERIC ANALYSIS OF THE STAR THETA URSAE MAJORIS

Major Field: Higher Education

Biographical:

Personal Data: Born at Mill Creek, Oklahoma, February 12, 1929, son of H. Z. Bulman and Eula Bulman.

Education: Graduated from Mill Creek High School in May 1947; received the Bachelor of Science degree from East Central State College in 1959, with a major in mathematics and physics; the Master of Science Degree from Oklahoma State University in 1964, with a major in Physics; completed the requirements for the Doctor of Education Degree in May, 1971.

Professional Experience: Employed as a physics teacher at Tulsa Central High School in 1959-60; Assistant Professor of Physics at East Central State College during 1961-70; Graduate Teaching Assistant, Oklahoma State University, Department of Physics, 1968.